Figure S1

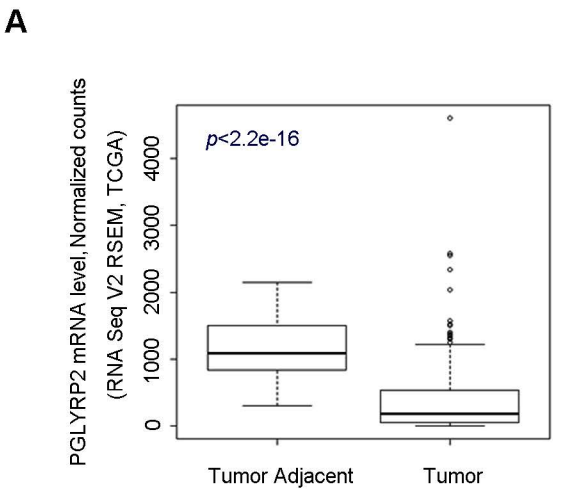
A
PGLYRP2 mRNA level,Normalized counts
(RNA Seq V2 RSEM, TCGA)
0
1000
2000
3000
4000
p<2.2e-16
Tumor Adjacent
Tumor

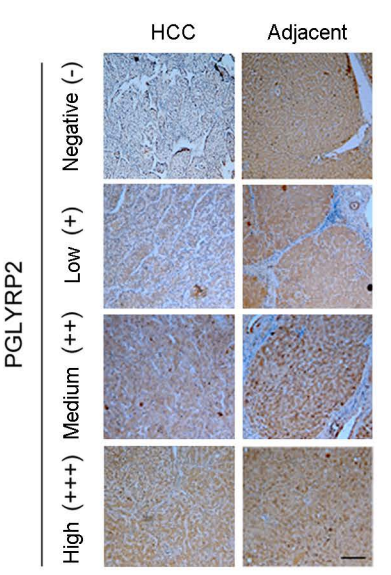
E
HCC
Adjacent
PGLYRP2
Negative (-)
Low (+)
Medium (++)
High (+++)

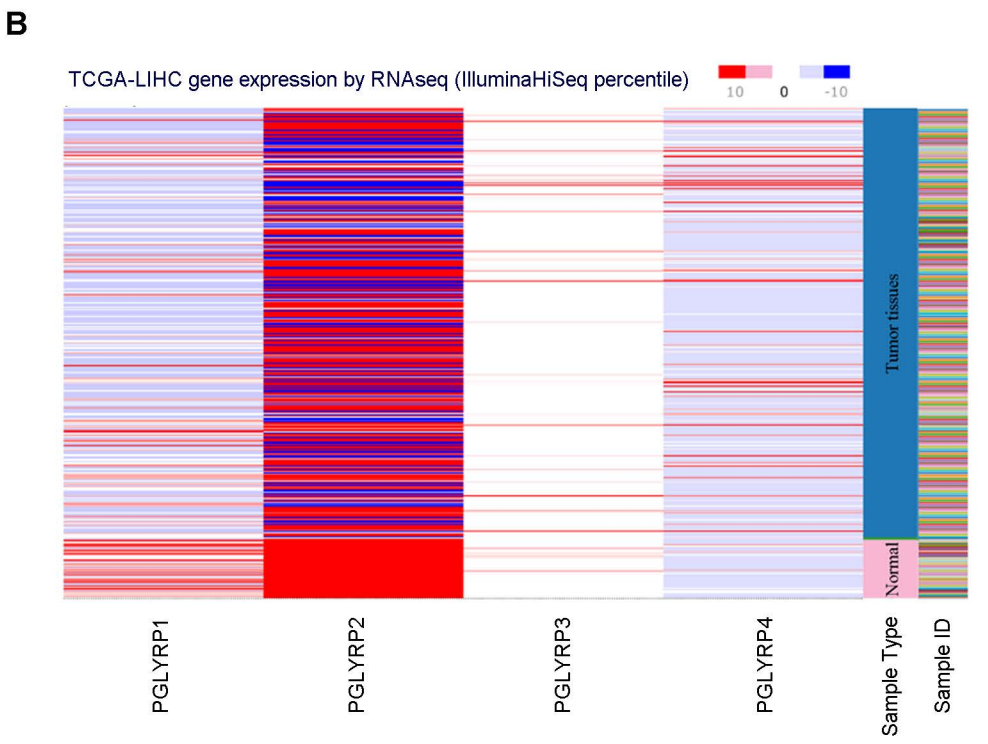
B
TCGA-LIHC gene expression by RNAseq (IlluminaHiSeq percentile)
10
0
-10
Tumor tissues
Normal
PGLYRP1
PGLYRP2
PGLYRP3
PGLYRP4
Sample Type
Sample ID

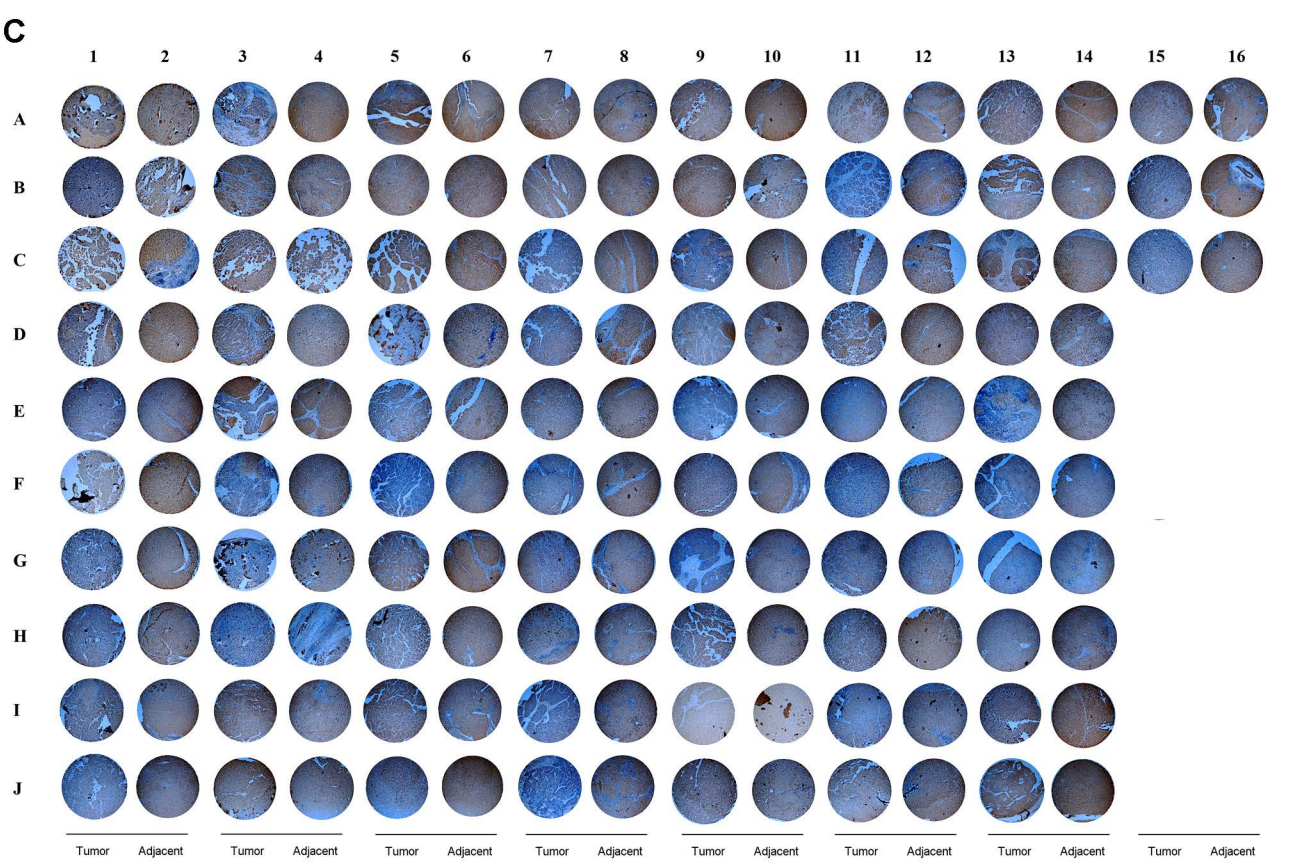
C
1 2 3 4 5 6 7 8 9 10 11 12 13 14 15 16
A
B
C
D
E
F
G
H
I
J
Tumor
Adjacent


D
1 2 3 4 5 6 7 8
A
B
C
D
Tumor
Adjacent
1 2 3 4 5 6
A
B
C
D
Tumor
Adjacent

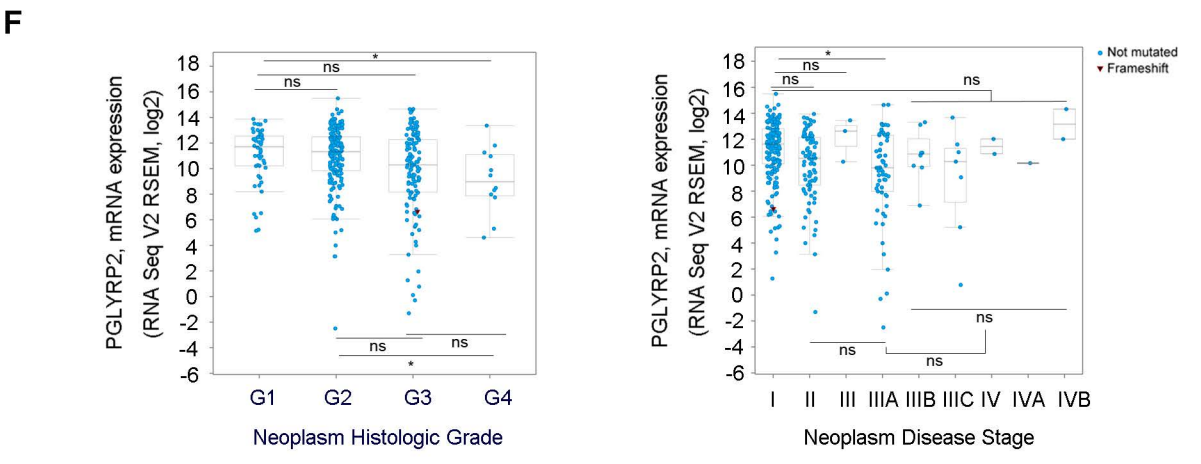
F
PGLYRP2, mRNA expression
(RNA Seq V2 RSEM, log2)
ns
*
G1
G2
G3
G4
Neoplasm Histologic Grade
Not mutated
Frameshift
I
II
III
IIIA
IIIB
IIIC
IV
IVA
IVB
Neoplasm Disease Stage

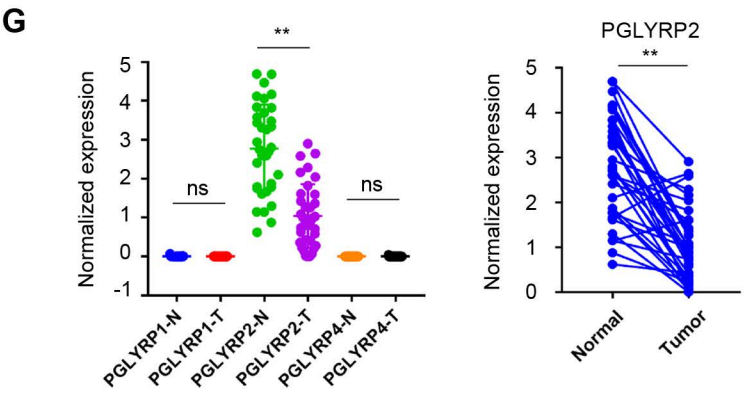
G
Normalized expression
**
ns
PGLYRP1-N
PGLYRP1-T
PGLYRP2-N
PGLYRP2-T
PGLYRP4-N
PGLYRP4-T
PGLYRP2
Normal
Tumor

Figure S2

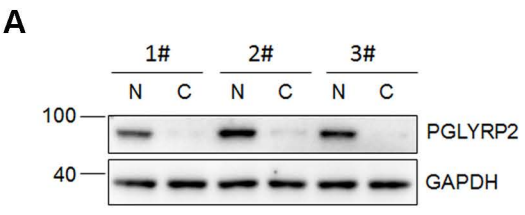
A
1#
2#
3#
N
C
N
C
N
C
100
40
PGLYRP2
GAPDH

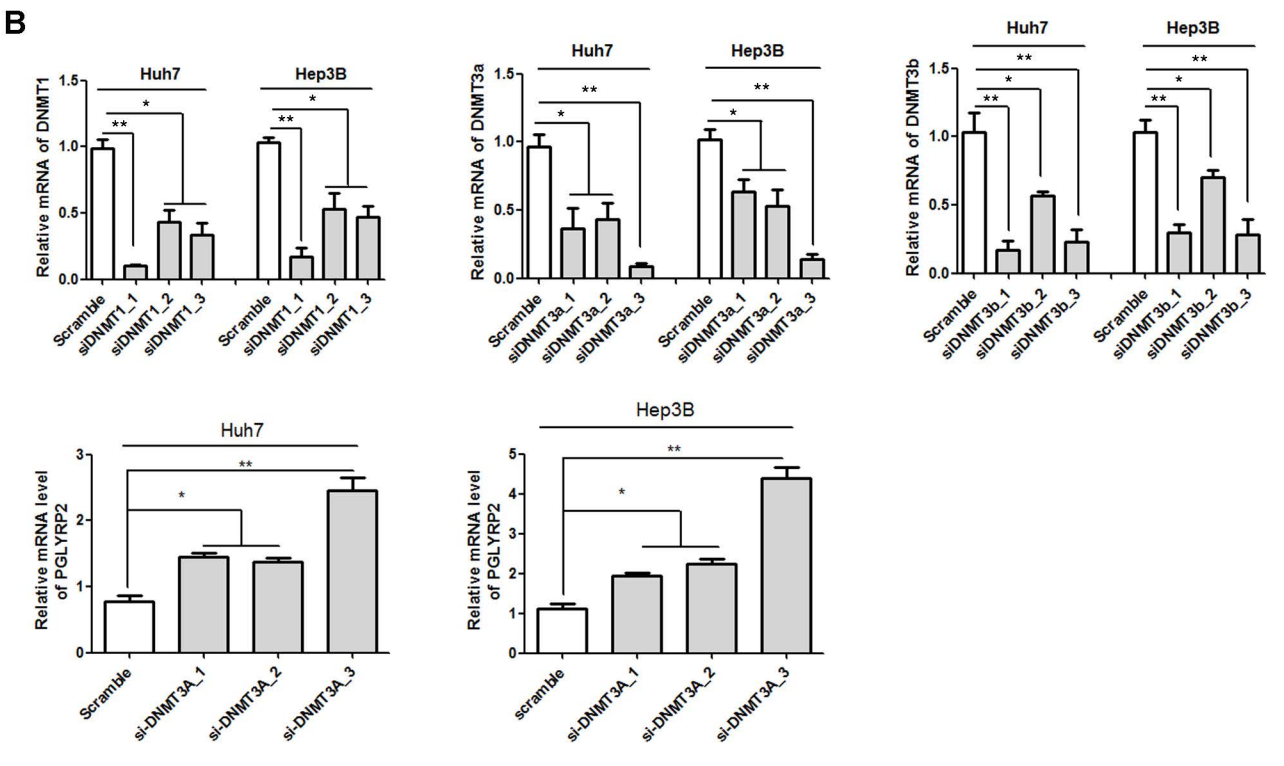
B
Huh7
Hep3B
Relative mRNA of DNMT1
Scramble
siDNMT1_1
siDNMT1_2
siDNMT1_3
Relative mRNA of DNMT3a
siDNMT3a_1
siDNMT3a_2
siDNMT3a_3
Relative mRNA of DNMT3b
siDNMT3b_1
siDNMT3b_2
siDNMT3b_3
Relative mRNA level of PGLYRP2
si-DNMT3A_1
si-DNMT3A_2
si-DNMT3A_3

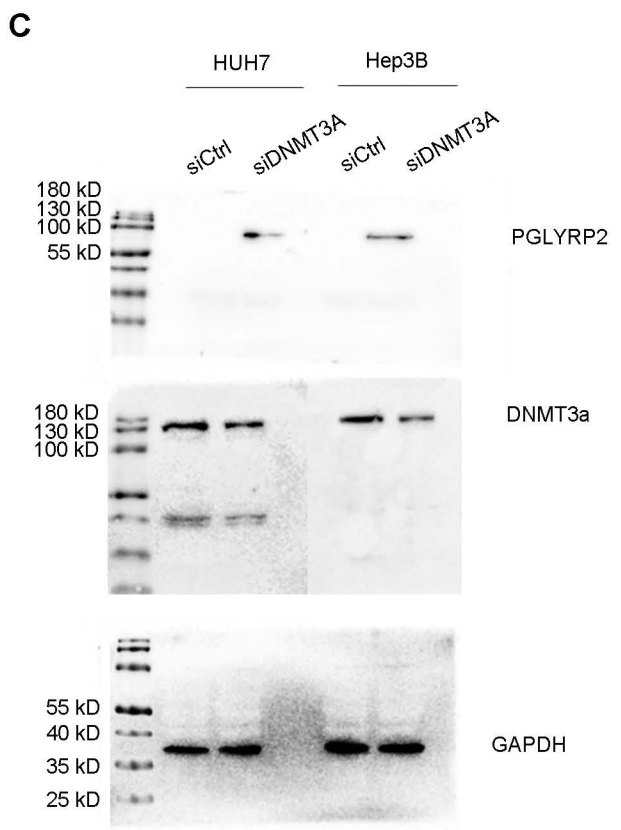
C
HUH7
Hep3B
siCtrl
siDNMT3A
180 kD
130 kD
100 kD
55 kD
PGLYRP2
DNMT3a
40 kD
35 kD
25 kD
GAPDH

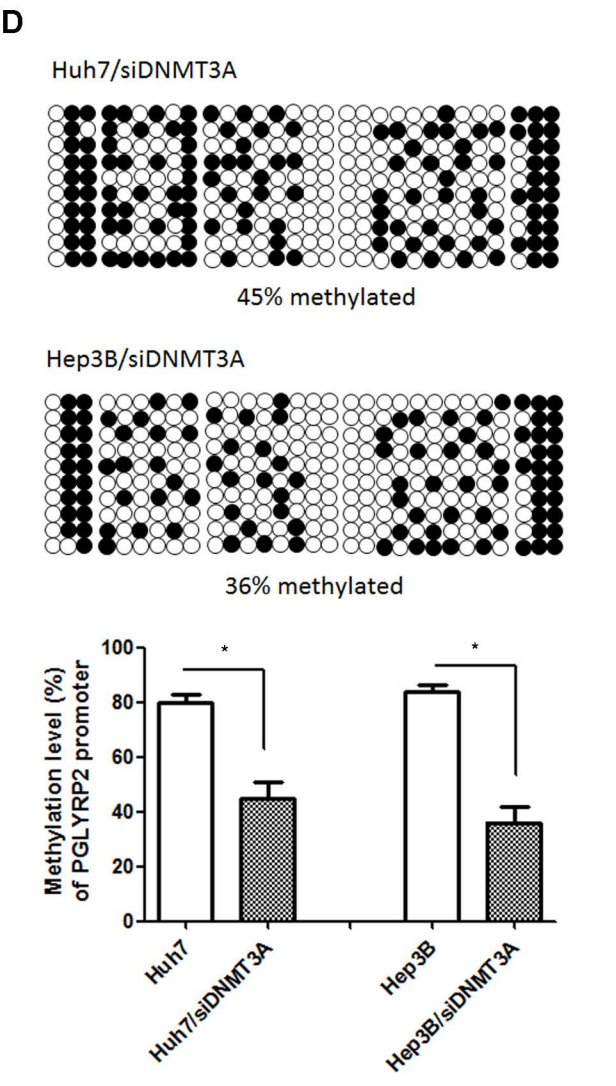
D
Huh7/siDNMT3A
45% methylated
Hep3B/siDNMT3A
36% methylated
Methylation level (%) of PGLYRP2 promoter
Huh7
Huh7/siDNMT3A
Hep3B
Hep3B/siDNMT3A

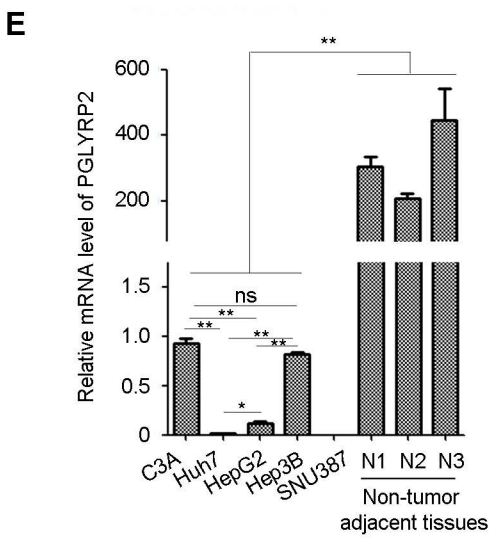
E
Relative mRNA level of PGLYRP2
ns
C3A
Huh7
HepG2
Hep3B
SNU387
N1
N2
N3
Non-tumor adjacent tissues

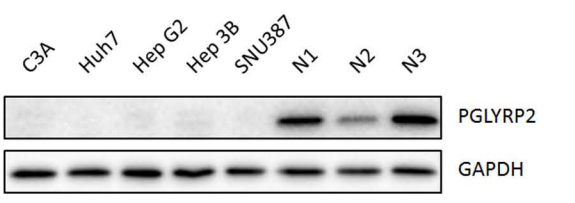
F
C3A
Huh7
Hep G2
Hep 3B
SNU387
N1
N2
N3
PGLYRP2
GAPDH

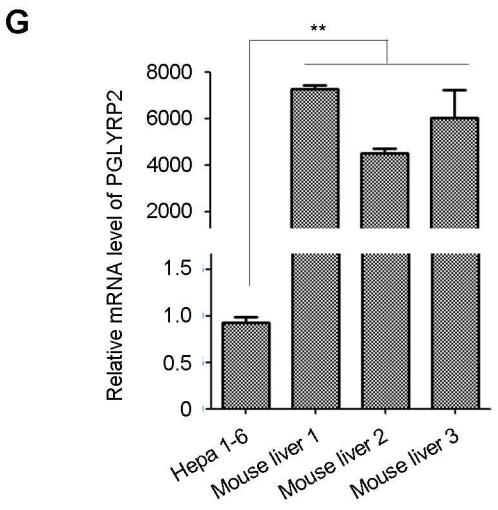
G
Relative mRNA level of PGLYRP2
Hepa 1-6
Mouse liver 1
Mouse liver 2
Mouse liver 3

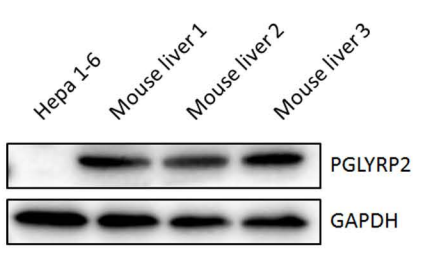
H
Hepa 1-6
Mouse liver 1
Mouse liver 2
Mouse liver 3
PGLYRP2
GAPDH

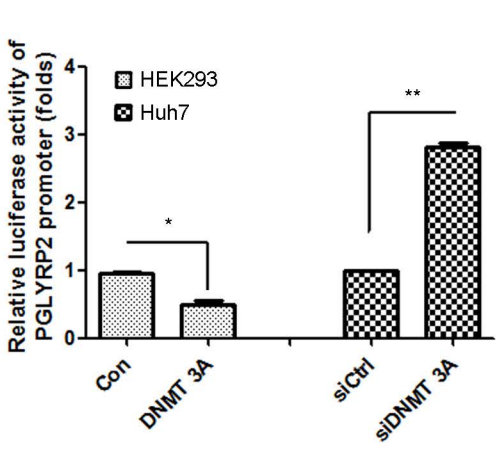
I
HEK293
Huh7
Relative luciferase activity of PGLYRP2 promoter (folds)
Con
DNMT 3A
siCtrl
siDNMT 3A

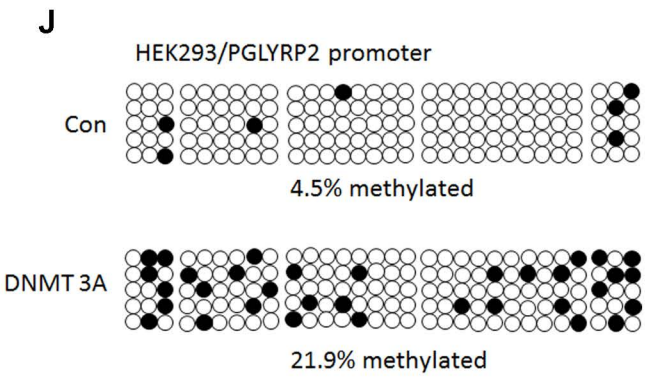
J
HEK293/PGLYRP2 promoter
Con
4.5% methylated
DNMT 3A
21.9% methylated

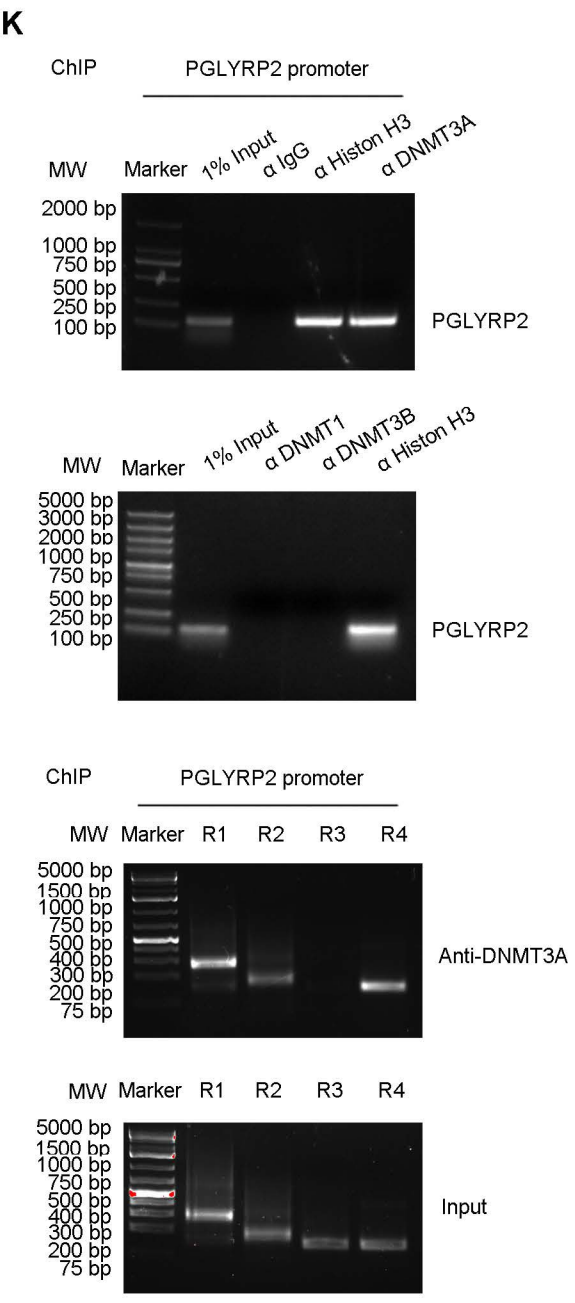
K
ChIP
PGLYRP2 promoter
MW
Marker
1% Input
α IgG
α Histon H3
α DNMT3A
PGLYRP2
α DNMT1
α DNMT3B
R1
R2
R3
R4
Anti-DNMT3A
Input

Figure S3

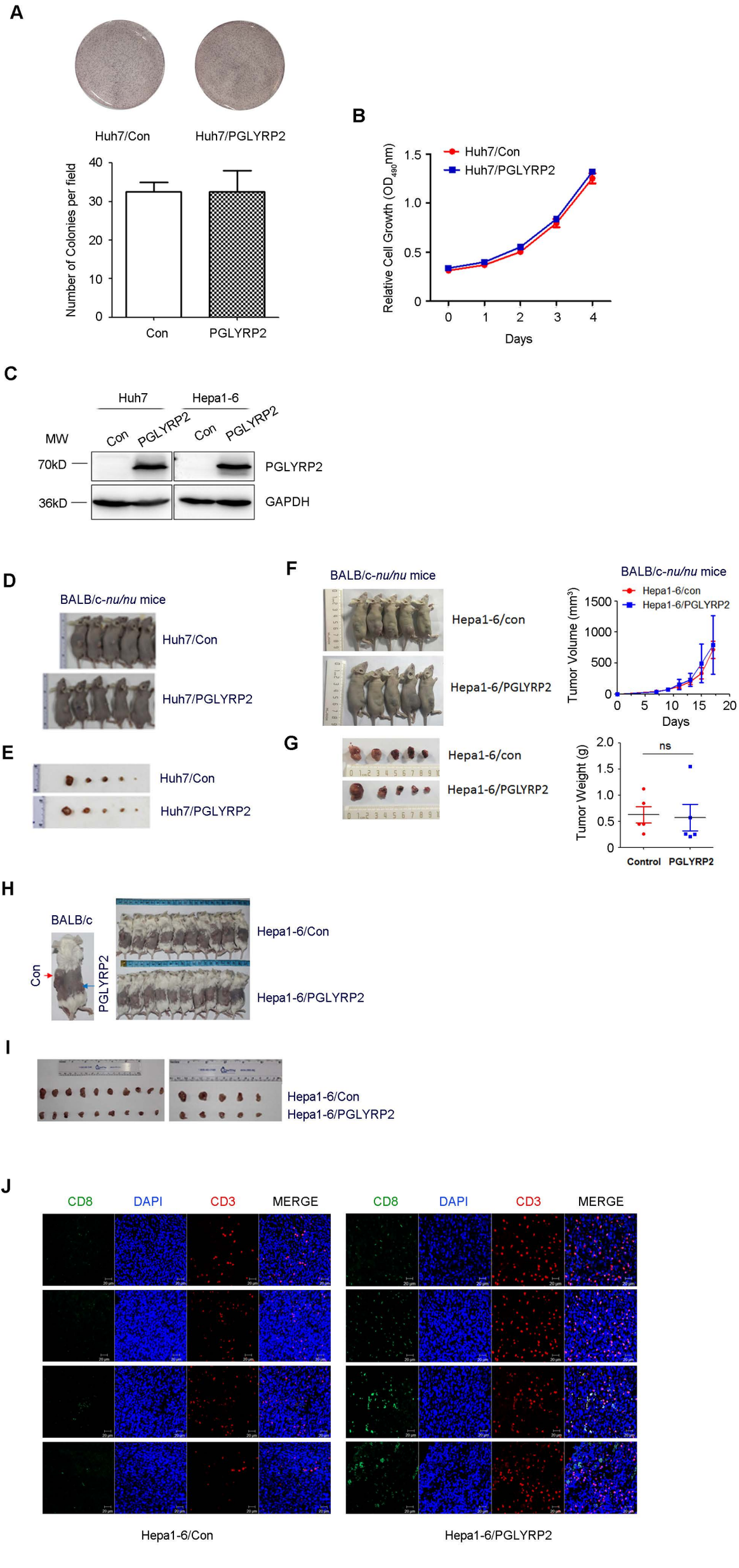
A
Huh7/Con
Huh7/PGLYRP2
Number of Colonies per field
40
30
20
10
0
Con
PGLYRP2
B
Huh7/Con
Huh7/PGLYRP2
Relative Cell Growth (OD490 nm)
1.5
1.0
0.5
0
0
1
2
3
4
Days
C
Huh7
Hepa1-6
MW
Con
PGLYRP2
Con
PGLYRP2
70kD
36kD
PGLYRP2
GAPDH
D
BALB/c-nu/nu mice
Huh7/Con
Huh7/PGLYRP2
E
Huh7/Con
Huh7/PGLYRP2
F
BALB/c-nu/nu mice
Hepa1-6/con
Hepa1-6/PGLYRP2
BALB/c-nu/nu mice
Hepa1-6/con
Hepa1-6/PGLYRP2
Tumor Volume (mm3)
1500
1000
500
0
0
5
10
15
20
Days
G
Hepa1-6/con
Hepa1-6/PGLYRP2
Tumor Weight (g)
2.0
1.5
1.0
0.5
0
ns
Control
PGLYRP2
H
BALB/c
Con
PGLYRP2
Hepa1-6/Con
Hepa1-6/PGLYRP2
I
Hepa1-6/Con
Hepa1-6/PGLYRP2
J
CD8
DAPI
CD3
MERGE
CD8
DAPI
CD3
MERGE
Hepa1-6/Con
Hepa1-6/PGLYRP2

Figure S4

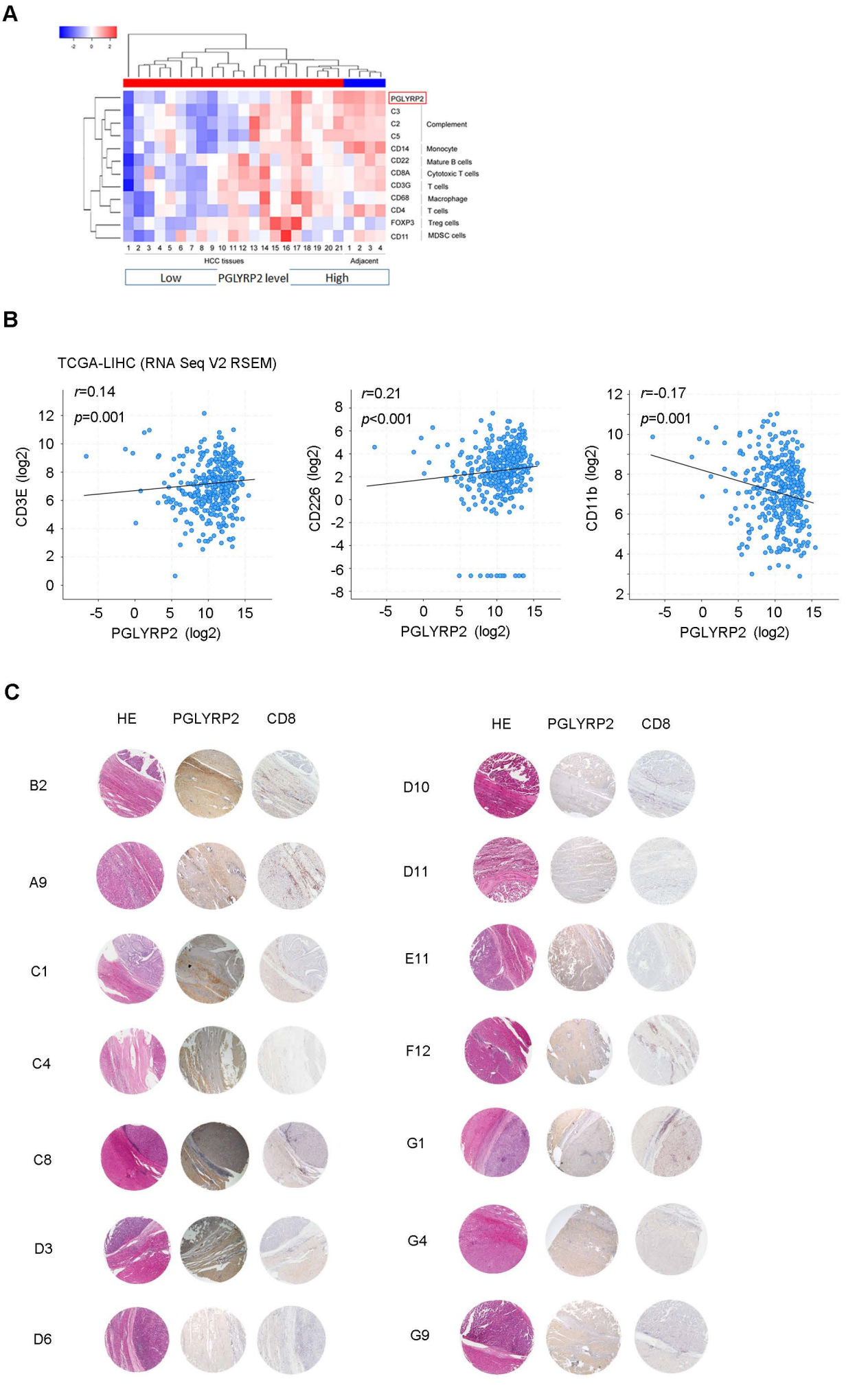
A
PGLYRP2
C3
C2
C5
Complement
CD14
Monocyte
CD22
Mature B cells
CD8A
Cytotoxic T cells
CD3G
T cells
CD68
Macrophage
CD4
T cells
FOXP3
Treg cells
CD11
MDSC cells
HCC tissues
Adjacent
Low
PGLYRP2 level
High
B
TCGA-LIHC (RNA Seq V2 RSEM)
r=0.14
p=0.001
CD3E (log2)
PGLYRP2 (log2)
r=0.21
p<0.001
CD226 (log2)
PGLYRP2 (log2)
r=-0.17
p=0.001
CD11b (log2)
PGLYRP2 (log2)
C
HE
PGLYRP2
CD8
B2
A9
C1
C4
C8
D3
D6
D10
D11
E11
F12
G1
G4
G9

Figure S5

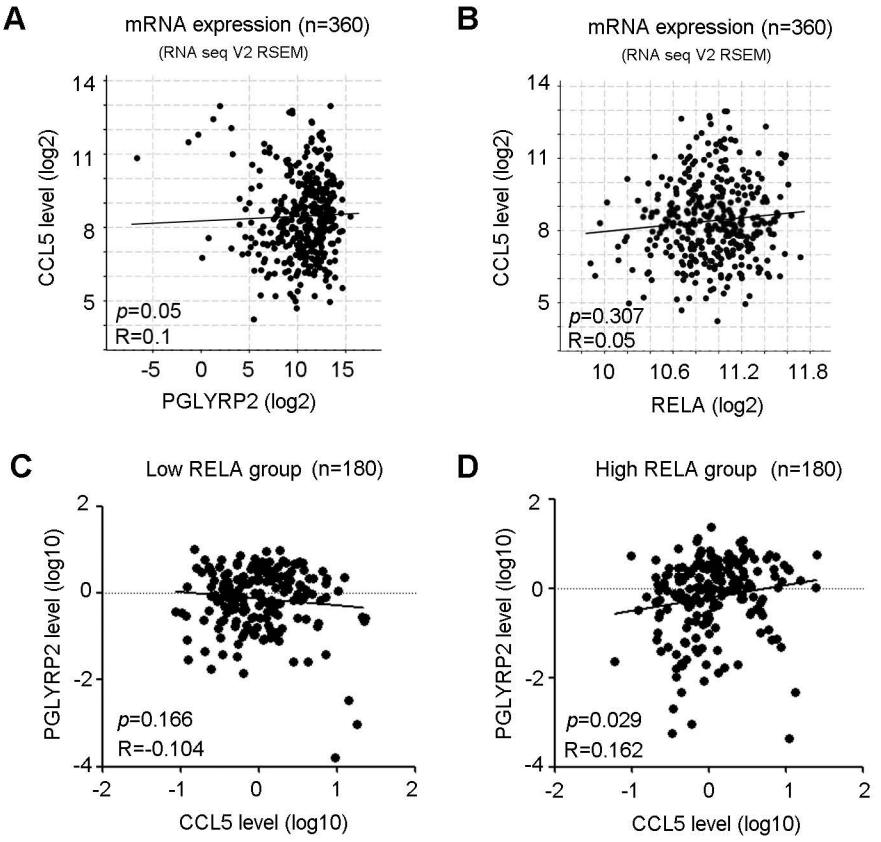
A
mRNA expression (n=360)
(RNA seq V2 RSEM)
CCL5 level (log2)
PGLYRP2 (log2)
p=0.05
R=0.1
B
mRNA expression (n=360)
(RNA seq V2 RSEM)
CCL5 level (log2)
RELA (log2)
p=0.307
R=0.05
C
Low RELA group (n=180)
PGLYRP2 level (log10)
CCL5 level (log10)
p=0.166
R=-0.104
D
High RELA group (n=180)
PGLYRP2 level (log10)
CCL5 level (log10)
p=0.029
R=0.162

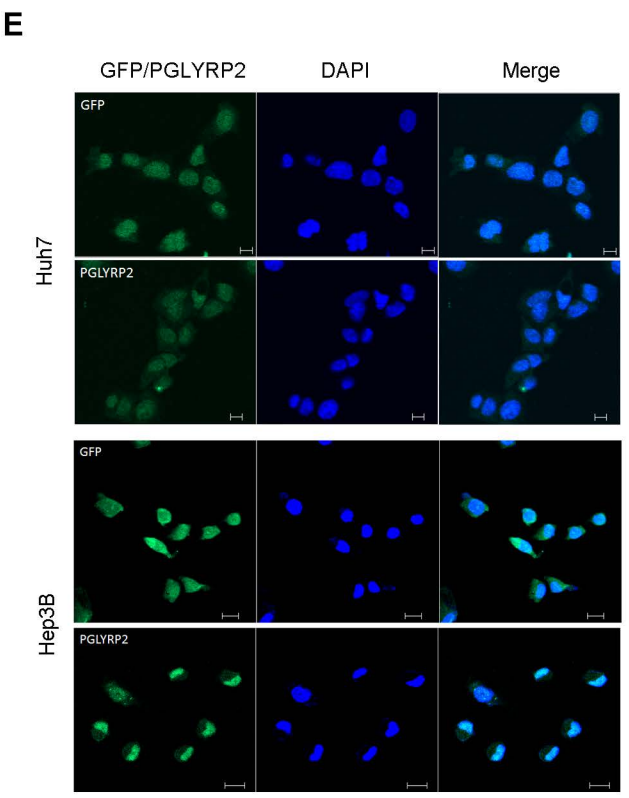
E
GFP/PGLYRP2
DAPI
Merge
Huh7
Hep3B
GFP
PGLYRP2

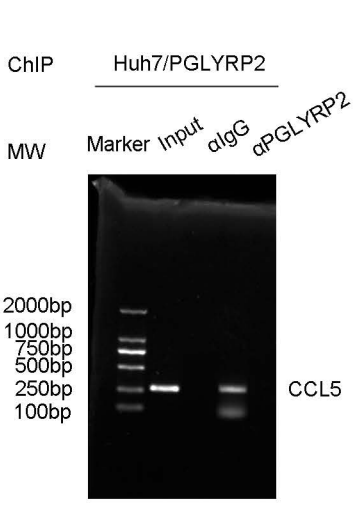
F
ChIP
Huh7/PGLYRP2
MW
Marker
Input
αIgG
αPGLYRP2
2000bp
1000bp
750bp
500bp
250bp
100bp
CCL5

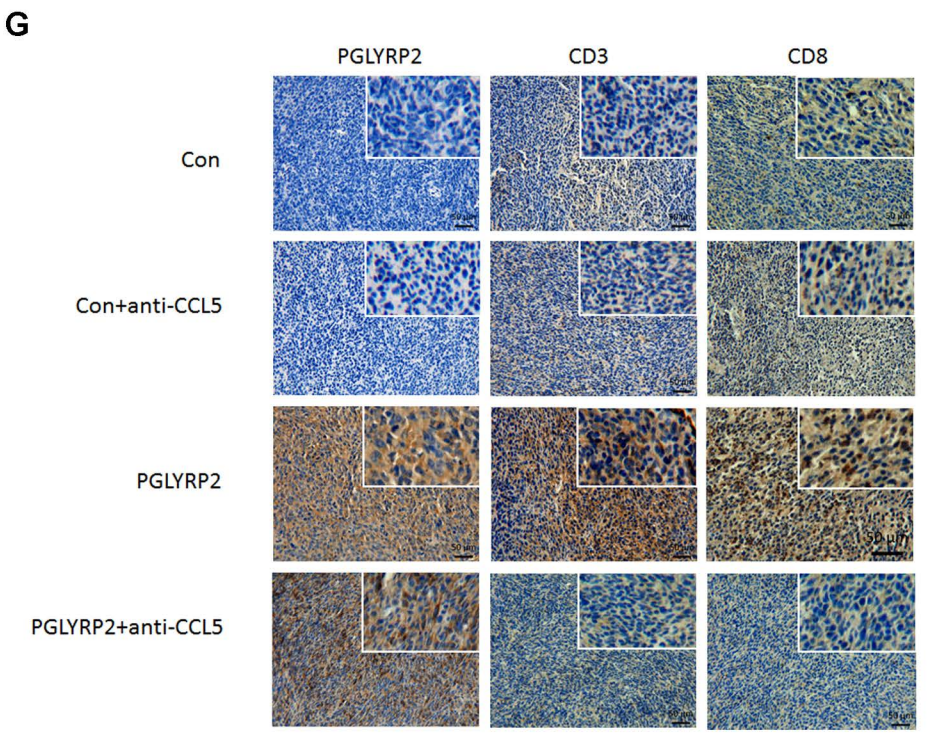
G
PGLYRP2
CD3
CD8
Con
Con+anti-CCL5
PGLYRP2
PGLYRP2+anti-CCL5

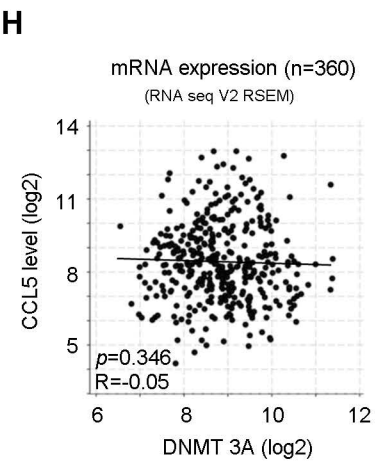
H
mRNA expression (n=360)
(RNA seq V2 RSEM)
CCL5 level (log2)
DNMT 3A (log2)
p=0.346
R=-0.05

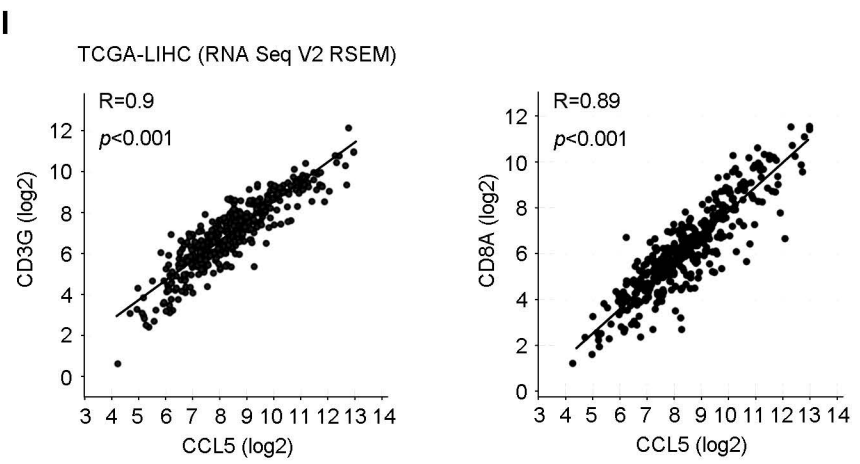
I
TCGA-LIHC (RNA Seq V2 RSEM)
R=0.9
p<0.001
CD3G (log2)
CCL5 (log2)
R=0.89
p<0.001
CD8A (log2)
CCL5 (log2)

Figure S6

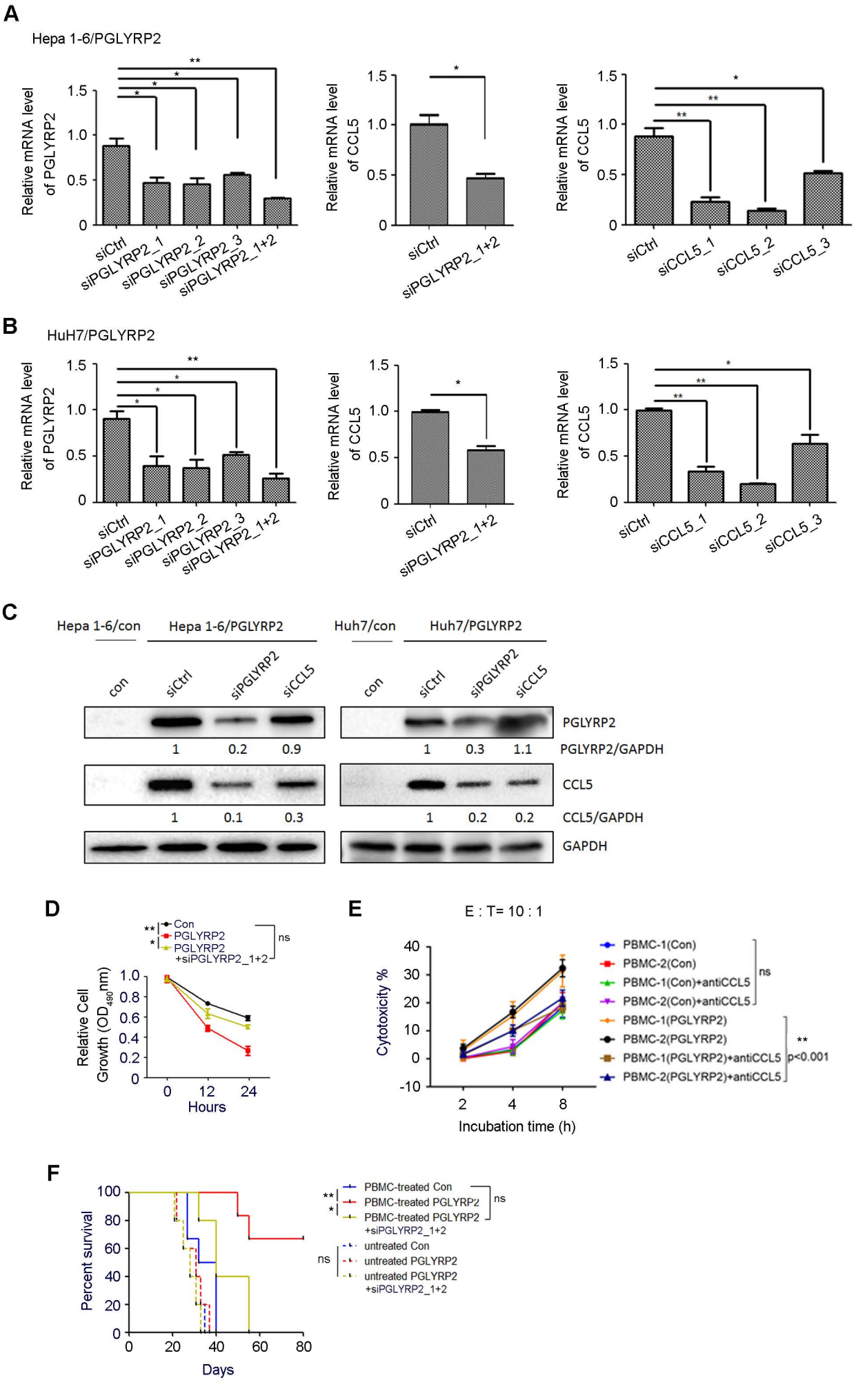
A
Hepa 1-6/PGLYRP2
Relative mRNA level of PGLYRP2
siCtrl
siPGLYRP2_1
siPGLYRP2_2
siPGLYRP2_3
siPGLYRP2_1+2
Relative mRNA level of CCL5
siCtrl
siPGLYRP2_1+2
Relative mRNA level of CCL5
siCtrl
siCCL5_1
siCCL5_2
siCCL5_3
B
HuH7/PGLYRP2
Relative mRNA level of PGLYRP2
siCtrl
siPGLYRP2_1
siPGLYRP2_2
siPGLYRP2_3
siPGLYRP2_1+2
Relative mRNA level of CCL5
siCtrl
siPGLYRP2_1+2
Relative mRNA level of CCL5
siCtrl
siCCL5_1
siCCL5_2
siCCL5_3
C
Hepa 1-6/con
Hepa 1-6/PGLYRP2
Huh7/con
Huh7/PGLYRP2
con
siCtrl
siPGLYRP2
siCCL5
PGLYRP2
1 0.2 0.9
1 0.3 1.1
PGLYRP2/GAPDH
CCL5
1 0.1 0.3
1 0.2 0.2
CCL5/GAPDH
GAPDH
D
Con
PGLYRP2
PGLYRP2 +siPGLYRP2_1+2
ns
Relative Cell Growth (OD490 nm)
Hours
E
E : T= 10 : 1
Cytotoxicity %
Incubation time (h)
PBMC-1(Con)
PBMC-2(Con)
PBMC-1(Con)+antiCCL5
PBMC-2(Con)+antiCCL5
ns
PBMC-1(PGLYRP2)
PBMC-2(PGLYRP2)
PBMC-1(PGLYRP2)+antiCCL5
PBMC-2(PGLYRP2)+antiCCL5
**
p<0.001
F
Percent survival
Days
PBMC-treated Con
PBMC-treated PGLYRP2
PBMC-treated PGLYRP2 +siPGLYRP2_1+2
ns
untreated Con
untreated PGLYRP2
untreated PGLYRP2 +siPGLYRP2_1+2
ns

Figure S7

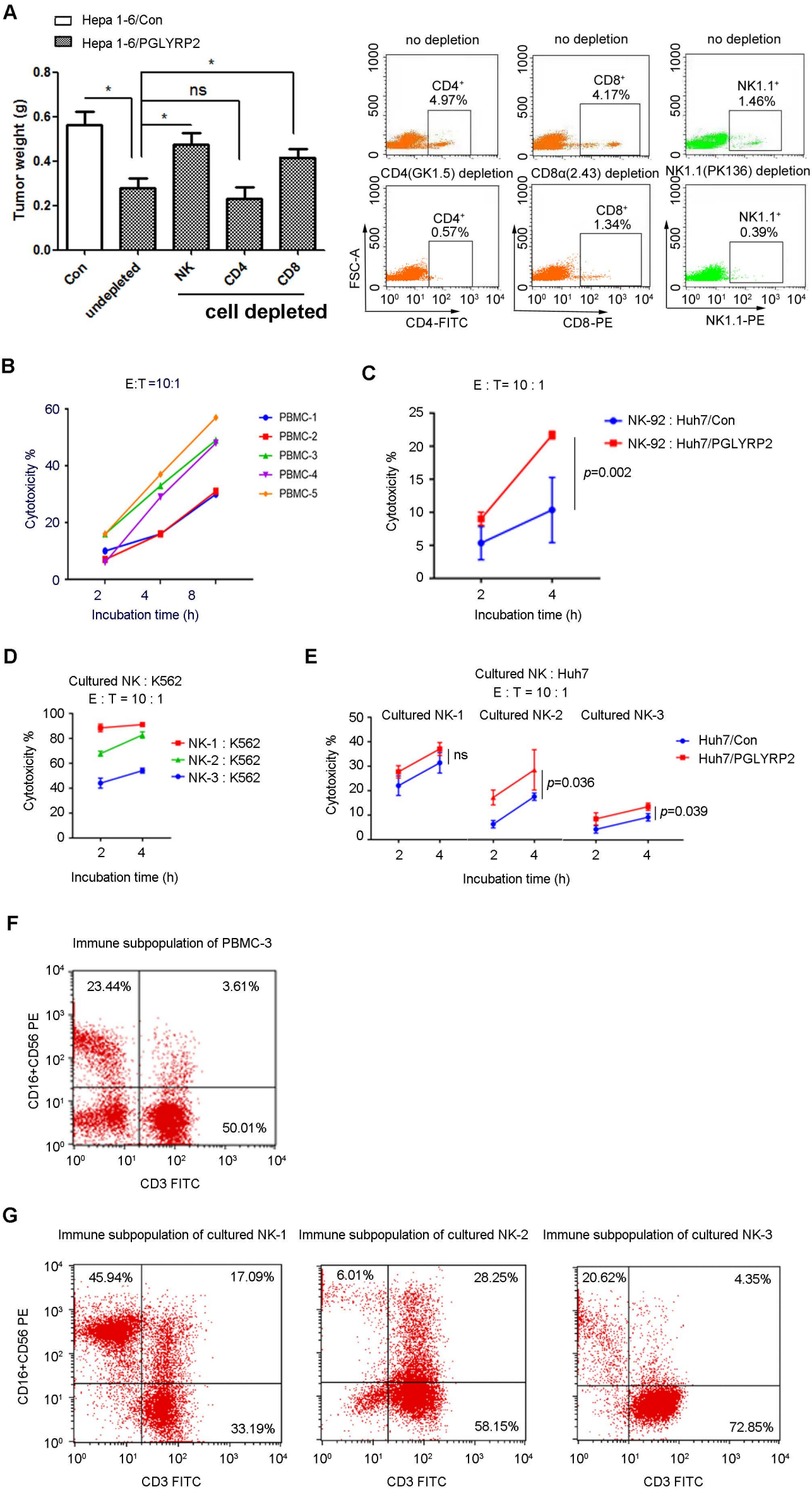
A
Hepa 1-6/Con
Hepa 1-6/PGLYRP2
Tumor weight (g)
Con
undepleted
NK
CD4
CD8
cell depleted
no depletion
CD4+ 4.97%
CD8+ 4.17%
NK1.1+ 1.46%
CD4(GK1.5) depletion
CD8α(2.43) depletion
NK1.1(PK136) depletion
CD4+ 0.57%
CD8+ 1.34%
NK1.1+ 0.39%
FSC-A
CD4-FITC
CD8-PE
NK1.1-PE
B
E:T =10:1
Cytotoxicity %
Incubation time (h)
PBMC-1
PBMC-2
PBMC-3
PBMC-4
PBMC-5
C
E : T= 10 : 1
NK-92 : Huh7/Con
NK-92 : Huh7/PGLYRP2
p=0.002
D
Cultured NK : K562
E : T = 10 : 1
NK-1 : K562
NK-2 : K562
NK-3 : K562
E
Cultured NK : Huh7
E : T = 10 : 1
Cultured NK-1
Cultured NK-2
Cultured NK-3
Huh7/Con
Huh7/PGLYRP2
ns
p=0.036
p=0.039
F
Immune subpopulation of PBMC-3
23.44%
3.61%
50.01%
CD16+CD56 PE
CD3 FITC
G
Immune subpopulation of cultured NK-1
Immune subpopulation of cultured NK-2
Immune subpopulation of cultured NK-3
45.94%
17.09%
33.19%
6.01%
28.25%
58.15%
20.62%
4.35%
72.85%

Figure S8

A

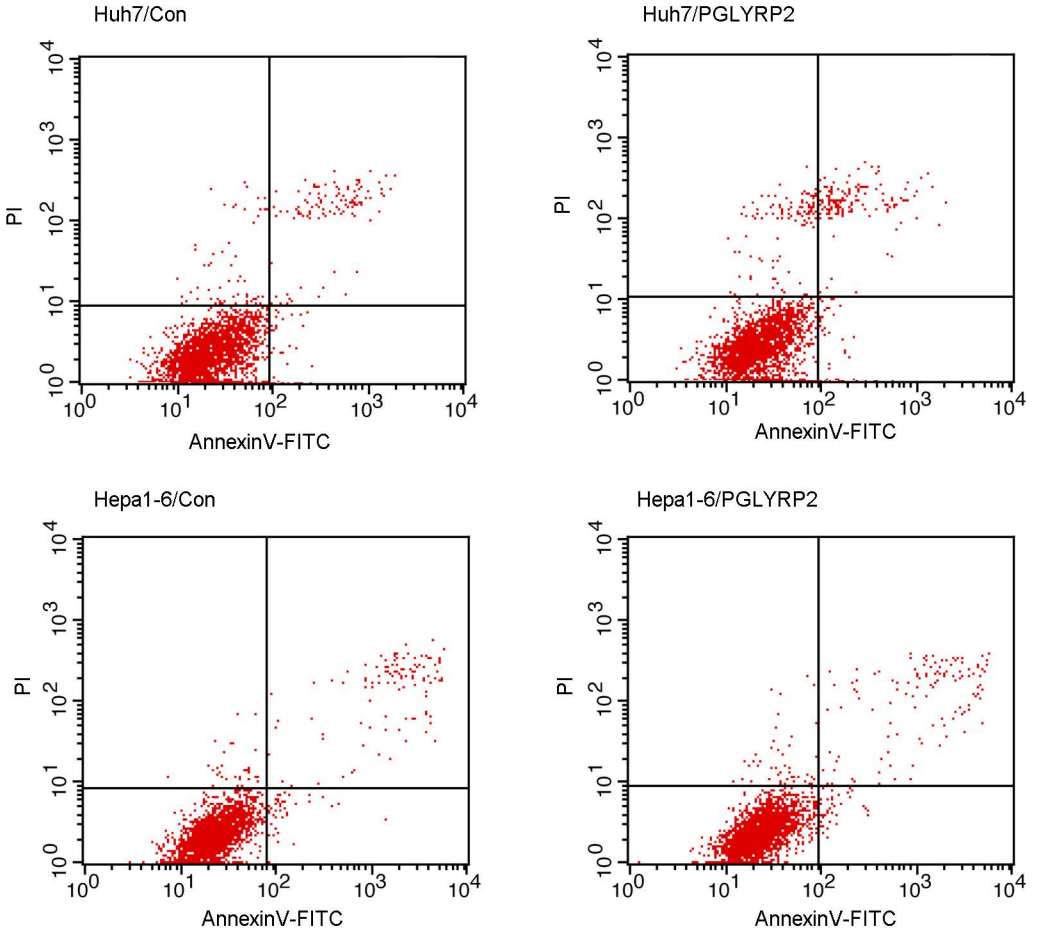
Huh7/Con
Huh7/PGLYRP2
Hepa1-6/Con
Hepa1-6/PGLYRP2
PI
AnnexinV-FITC

B

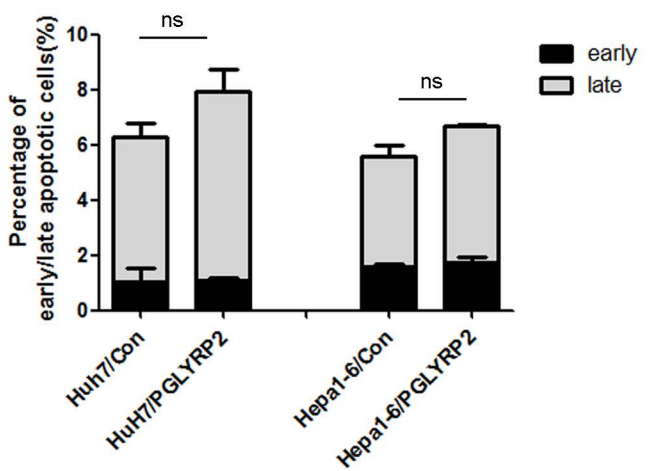
Percentage of early/late apoptotic cells(%)
ns
ns
early
late
Huh7/Con
HuH7/PGLYRP2
Hepa1-6/Con
Hepa1-6/PGLYRP2

Tumor-Derived PGLYRP2 Predicts Survival and Antitumor Immune Responses in Hepatocellular Carcinoma

Zongyi Yang, Jia Feng, Li Xiao, Xi Chen, Yuanfei Yao, Yiqun Li, Yu Tang, Shuai Zhang, Min Lu, Yu Qian, Hongjin Wu* & Ming Shi*

Table of contents

Supplementary Methods

Patient samples

Ninety-eight paired tumor-adjacent non-cancerous liver tissues and HCC tissue samples and additional fourteen HCC tissues were from human liver cancer tissue array HLiv-HCC180Sur-01, Hliv-HCC030PG-01, HLivH090Su01 and OD-CT-DgLiv02-005 (Outdo Biotech, Shanghai, China). Twenty-two paired cDNA of HCC tissues and their corresponding adjacent non-tumor tissues were from human liver cancer cDNA array cDNA-HlivH60PG02 (Outdo Biotech, Shanghai, China). The collection of three HCC samples used for bisulfite sequencing, patient consent, and patient recruitment followed Institutional Review Board protocols from the First Affiliated Hospital of Kunming Medical University. The clinical information of these liver cancer tissues were listed in Table S2. The study has been approved by the Research Ethics Committee of Harbin Institute of Technology and the First Affiliated Hospital of Kunming Medical University.

Chemokine analysis

The tissue lysates of high PGLYRP2-expressing HCC tissue and low PGLYRP2-expressing HCC tissue were obtaining by homogenizing tissue in homogenization buffer (10 mM HEPES-KOH (pH 7.6), 25 mM KCl, 0.15 mM spermine, 0.5 mM spermidine, 2 M sucrose, 10% (v/v) glycerol, 1 mM EDTA

(pH 8.0)). Cell culture supernates of Huh7/Con and Huh7/PGLYRP2 were harvested after 24 h of culture and frozen at −80°C until further analyses. Sample protein concentration was quantified using BCA protein concentration determination kit (Beyotime, Jiangsu, China). The concentrations of chemokines were measured with a human chemokine array kit (R&D Systems, Minneapolis, MN, USA) according to the manufacturer's instructions.

Human tumor xenograft, immune-competent syngeneic murine tumor model and orthotopic HCC mouse model

All animal procedures were performed according to protocols approved by the Rules for Animal Experiments published by the Chinese Government (Beijing, China) and approved by the Research Ethics Committee of Harbin Institute of Technology, China. Animals were housed in micro-isolator cages, including a wire rack in the cage for holding food and a water bottle. Animals were housed on a 12 h light/dark cycle. PGLYRP2-transfected human hepatoma cell line HuH7 stable cells and control cells were injected intraperitoneally or subcutaneously into the right posterior flanks of 6-week-old BALB/c nude mice (female, five mice per group). PGLYRP2-transfected mouse hepatoma cell line Hepa 1-6 stable cells and control cells were injected subcutaneously into the right posterior flanks of 6-week-old immune-competent BALB/c mice (female, ten mice per group). Tumor growth was assessed using standard caliper measurement twice a week. The following formula was used to calculate tumor

volume: Tumor volume (mm3)=(tumor length × width^2)/2, with all measurements in mm. Following 25-40 days of treatment, mice were sacrificed and tumor tissues were harvested. Then the subcutaneous tumor was cut into cubes 1 mm^3 in size, and implanted into the liver of each group respectively to mimic the primary HCC (6 mice in each group). After 2 weeks of implantation, the mice were sacrificed, and the size of tumors was calculated and compared as mentioned above.

Quantitative real-time PCR and Western blot analysis

Quantification of mRNA level was performed in a 20 μl mixture consisted of 10 μl 2×SYBR Green Mix, 0.2 ml RT product, 1 μl primer set mix at a concentration of 5 pmol/ml for each primer and 8.8 μl sterile water. As internal control, GAPDH mRNA was performed in same condition except the primer. The experiment was set on ABI 7500 Real-time PCR System (Foster City, CA, USA), PCR program was according to protocol's recommendation (10 minutes at 95 ℃ for 1 cycle, 10 seconds at 95 ℃, 34 seconds at 60 ℃ and 30 seconds at 72 ℃ for 40 cycles, 10 minutes at 72 ℃ for 1 cycle). Primers for qPCR are described in Supplementary Table S3.

Cells were collected and lysed in RIPA lysis buffer (150 mm NaCl, 50 mm Tris (pH 8.0), 0.5 mm EDTA, and 1% Nonidet P-40) plus complete protease inhibitor mixture (Roche Applied Science, Indianapolis, USA). The protein levels were determined using western blot analysis, as previously reported(1).

Immunohistochemical analysis and Immunofluorescence Staining

The immunohistochemical staining was performed as described previously(2). Antibody against PGLYRP2 (#NBP2-32042) was purchased from Novus Biologicals. Immunofluorescence staining was performed as described previously(1). For the analysis of T cell infiltration in the paraffin-embedded tumor tissue, immunofluorescence staining of T cells was performed. Primary antibodies against mouse CD3 and CD8 (Cell Signaling Technology, Massachusetts, USA) were used. The secondary antibodies used were goat anti-rabbit IgG and anti-rat IgG (Invitrogen, Carlsbad, CA, USA). Images were analyzed with a Zeiss Axioskop-2 microscope. 488 and 633 nm wavelength lasers were used to excite Fluorescein tags. DAPI was excited by UV light.

Bisulfite DNA sequencing

Bisulfite DNA sequencing was conducted as described previously.(2) Briefly, bisulfite modification of DNA was performed by following the protocol of Applied Biosystems methylSEQr Bisulfite Conversion kit. Bisulfite-treated DNA was amplified using nest PCR with primers described in Supplementary information, Table S3. Amplified bisulfite-treated DNA was sequenced and compared with original sequence of *PGLYRP2* gene.

In vivo mAb treatment

Mice were injected intraperitoneally or subcutaneously with various amounts of

antibodies. Immune cell subsets were depleted by intraperitoneally administering 200 μg of depleting antibody i.p. twice weekly beginning one day prior to experiments as indicated: CD8 T-cells with anti-CD8α (clone 2.43, BioXCell, West Lebanon, NH, USA), CD4 T-cells with anti-CD4 (clone GK1.5, BioXCell, West Lebanon, NH, USA), NK cells with anti-NK1.1 (clone PK136, BioXCell, West Lebanon, NH, USA). CCL5 was blocked by intratumoral administrating 20 μg of anti-CCL5 blocking antibody (53405.111, ab10394, Abcam, Cambridge, UK) at 3rd , 5th and 7th day after tumor injection.

Luciferase assay and MTT assay

Luciferase assay was performed as described previously(1). Cells were transfected with promoter luciferase reporter plamids using Lipofectamine 2000 (Invitrogen, Carlsbad, CA, USA). Luciferase assays were performed by using the luciferase assay system (Promega, Madison, WI, USA); b-Galactosidase activity was used as an internal control. Luciferase activity was measured by using CytoFluorplate 4000 Luminescence Microplate Reader (ABI, Foster City, CA, USA).

Cell viabilities were assessed by a MTT [3-(4,5-dimethylthiazol-2-yl) -2,5-diphenyltetrazolium bromide] (Sigma-Aldrich, Milwaukee, USA) assay. Briefly, MTT solution in DMEM containing 10% FBS was added to each well at the final concentration of 0.5 mg/mL. The cells were incubated for 4 h at 37°C. The MTT medium was aspirated and then 100 μl dimethylsulfoxide (DMSO, Sigma-

Aldrich, Milwaukee, USA) was added. Optical density was measured with a spectrometer at 490 nm. Each experiment was conducted in triplicates and repeated independently for 3 times.

Cell viability and cell cytotoxicity assays

Cell viability was assessed by the MTT Cell Viability Assay Kit (Beyotime, Jiangsu, China). Cell cytotoxicity of PBMCs was assessed by measuring fluorescence intensity of green-fluorescent Calcein AM (#C3099; Thermo Fisher Scientific, Waltham, MA, USA) in intact tumor cells. Briefly, target cells (tumor cells) were resuspend with DMEM medium containing 10%FBS, and mixed with 20 μl Calcein AM at 37℃, 30min for staining. PBMCs were co-cultured with pre-stained target cells at a certain E:T ratio for 2 h, 4 h or 8 h of incubation time. The fluorescence intensity of living target cells is measured by using Terascan VPC instrument (Minerva Tech, Tokyo, Japan). Percent cytotoxicity of the assay was calculated by the following formula: % cytotoxicity = (1-[(average fluorescence of the sample wells - average fluorescence of the maximal release control wells)/(average fluorescence of the minimal release control wells - average fluorescence of the maximal release control wells)]) ×100 (3).

Chromatin Immunoprecipitation (CHIP)

ChIP assay was performed as described previously(4). 1×10^7 Huh7 cells were

cross-linked with 1 % formaldehyde for 10 min and then neutralized with 125 mM glycine for 5 min. Cells were collected by centrifugation (2,000 g for 5 min at 4 °C) and washed twice with ice-cold PBS. Cells were lysed in 150 µl Buffer A (10 mM Tris–HCl, pH 8.0, 10 mM NaCl, 0.2 % NP40) for 10 min on ice and cell pellet was collected and resuspended in 1 ml Buffer B (50 mM Tris–HCl, pH 8.0, 10 mM EDTA, 1 % SDS). The lysate was fragmented by sonication to yield fragments between 500 bp and 1000 bp, and then centrifuged at 13,000 g for 15 min at 4°C. The supernatant was whole cell lysates. 5 µg of antibody against Histon H3, DNMT 3A or PGLYRP2 (Abcam, Cambridge, MA) was added into the tubes containing 200 µl whole cell lysate plus 300 µl Buffer C (16.7 mM Tris–HCl, pH 8.0, 167 mM NaCl, 1.2 mM EDTA, 0.01 % SDS, 1.1 % Triton X-100). After incubation for 4 h, the antigen-antibody complexes were collected with protein A agarose beads and subjected to serial washes. Cross-linked chromatin was reversed at 65°C in the presence of 200 mM NaCl for 5 h. The DNA fragments were then purified using chloroform-isoamyl alcohol, and were amplified by using PCR with specific primers (Table S3). PCR products were then run on agarose gel and photographed.

Supplementary information, Figure Legends

Fig. S1 PGLYRP2 level is decreased in HCC tissues and the downregulated level of PGLYRP2 correlates with poor prognosis in patients with HCC. (A) PGLYRP2 mRNA levels were analyzed in tumor-adjacent non-cancerous liver tissues and HCC tissues from TCGA-LIHC. (B) mRNA levels of PGRP family members were analyzed in tumor-adjacent non-cancerous liver tissues and HCC tissues from TCGA-LIHC. (C, D) Expression levels of PGLYRP2 protein in 73 paired tumor-adjacent non-cancerous liver tissues and HCC tissue samples from human liver cancer tissue array HLiv-HCC180Sur-01 (C), 15 paired tumor-adjacent non-cancerous liver tissues and HCC tissue samples from human liver cancer tissue array Hliv-HCC030PG-01 (left panel, D) and 10 paired tumor-adjacent non-cancerous liver tissues and HCC tissue samples from human liver cancer tissue array OD-CT-DgLiv02-005 (right panel, D) were evaluated using immunohistochemistry assay. (E) Immunohistochemistry results showed different intensities of PGLYRP2 protein expression in paired tumor-adjacent non-cancerous liver tissues and HCC tissues. (F) The relationship between PGLYRP2 level and neoplasm grades (left), stages (right) in patients of TCGA-LIHC were analyzed. (G) Relative protein levels of PGLYRP1, PGLYRP2 and PGLYRP4 in HCC tissues and tumor-adjacent non-cancerous liver tissues were analyzed according to the LC-MS/MS-based proteomic data from Chinese Human Proteome Project (CNHPP). The results are reported as mean ± SEM. *, $p<0.05$; **, $p<0.001$; ns,

not significant.

Fig. S2 DNMT3A-mediated promoter hyper-methylation results in downregulation of PGLYRP2 in HCC. (A) The expression levels of PGLYRP2 in the three HCC tissues used for bisulfite sequencing were detected by Western blot. (B) The levels of DNMT 1, DNMT 3A, DNMT 3B and PGLYRP2 were detected in Huh7 and Hep3B transfected with scramble siRNA, DNMT 1 siRNA, DNMT 3a siRNA or DNMT 3b siRNA alone by using Real-time PCR. (C) The levels of PGLYRP2 and DNMT 3A in DNMT 3A knockdowned Huh7 or Hep3B cells were detected by Western blotting. (D) Methylation status of the PGLYRP2 promoter region was analyzed in Huh7/siDNMT 3A and Hep3B/siDNMT 3A cells. The methylation levels of PGLYRP2 promoter in Huh7, Huh7/siDNMT 3A, Hep 3B and Hep3B/siDNMT 3A cells were analyzed. (E, F) PGLYRP2 expression levels were detected in human HCC cell lines C3A, Huh7, HepG2, Hep3B, SNU387 by Real-time PCR (E) and Western blot (F). Three human non-tumor adjacent tissues acted as controls. (G, H) PGLYRP2 expression level was detected in mouse HCC cell line Hepa 1-6 by Real-time PCR (G) and Western blot (H). Three mouse normal liver tissues acted as controls. (I) Luciferase activity of PGLYRP2 promoter was detected in DNMT3A-overexpressed HEK293/PGLYRP2 promoter luciferase reporter cells and DNMT 3A-silenced Huh7cells. (J) The methylation status of the PGLYRP2 promoter region was analyzed in Con or DNMT3A-overexpressed

HEK293/PGLYRP2 promoter luciferase reporter cells. (K) The binding activity of DNMT1, DNMT3A and DNMT3B to PGLYRP2 promoter was assessed by ChIP assay in Huh7 cells. Four regions in PGLYRP2 promoter were chosen to analyze the DNMT3A binding regions in ChIP assay. The four regions of PGLYRP2 promoter were R1, -1741 to -1491; R2, -1516 to -1362; R3, -736 to -614; R4, -440 to -315. All the results are reported as mean ± SEM. *, $p<0.05$; **, $p<0.001$; ns, not significant.

Fig. S3 PGLYRP2 suppresses HCC progression in immunocompetent mice and promotes antitumor immune response. (A) Cell colony formation assay was performed in Huh7/Con and Huh7/PGLYRP2 cells. Number of cell colonies was counted every 5 cm^2 field. (B) MTT assay was carried out in Huh7/Con and Huh7/PGLYRP2 cells. (C) PGLYRP2 expression in Huh7/PGLYRP2, Hepa1-6/PGLYRP2 and corresponding control cells was examined by Western blotting. (D, E) Human cancer cells Huh7/con or Huh7/PGLYRP2 were subcutaneously injected (s.c.) into BALB/c-*nu/nu* mice (D). Tumor weight was measured at 30 days after injection (E). (F, G) Murine cancer cells Hepa1-6/con or Hepa1-6/PGLYRP2 cells were inoculated s.c. in BALB/c-*nu/nu* mice (F). Tumor weight was measured at the end of the sudy (G). (H, I) Murine cancer cells Hepa1-6/con or Hepa1-6/PGLYRP2 cells were inoculated s.c. in immune-competent BALB/c mice (H). Tumor weight was measured at the end of the sudy (I). (J) Immunofluorescent staining of CD3 and

CD8 were performed on paraffin-embedded tumor tissue with Hepa1-6/Con or Hepa1-6/PGLYRP2. All the results are reported as mean ± SEM. The ns indicates there is no significant difference.

Fig. S4 PGLYRP2 expression level was correlated with tumor-infiltrating lymphocytes in HCC. (A) The expression of PGLYRP2 and immune cell markers were detected in 22 HCC samples using RT-qPCR array assay. Heat map showed different expression of PGLYRP2 and immune cell markers in 22 HCC tissues. (B) The association between PGLYRP2 mRNA level and immune cell markers in TCGA-LIHC cohort was analyzed. The markers included CD3E (total T cells), CD226 (activated T cells, NK cells and NKT cells) and CD11b (MDSCs). (C) HE staining of 14 HCC samples and immunohistochemistry assays of PGLYRP2 and CD8 in HCC tissues were shown.

Fig. S5 The association between CCL5 and PGLYRP2 level in HCC. (A) The association between CCL5 and PGLYRP2 mRNA levels in TCGA-LIHC was analyzed (n=360). (B) The association between CCL5 and RELA mRNA levels in TCGA-LIHC was analyzed (n=360). (C, D) The TCGA samples were split into high RELA and low RELA expression groups (50%, n=180); In low RELA group (C) and high RELA group (D), the correlation between CCL5 and PGLYRP2 was analyzed respectively. (E) Localization of PGLYRP2 in Huh7/PGLYRP2 (upper panel) and Hep3B/PGLYRP2 (lower panel) cells was examined using

immunofluorescence assay. (F) The binding activity of PGLYRP2 to CCL5 promoter was assessed by ChIP assay in Huh7/PGLYRP2 cells. (G) Immunohistochemistry assays showed PGLYRP2, CD3 and CD8 protein expression in HCC tissues. (H) The association between CCL5 and DNMT 3A mRNA levels in TCGA-LIHC was analyzed (n=360). $P > 0.05$ indicates that there is no significant difference. (I) The association between CCL5 and CD3G/CD8A mRNA levels in TCGA-LIHC was analyzed (n=360).

Fig. S6 PGLYRP2/CCL5 axis regulates tumor immunity. (A, B) PGLYRP2 or CCL5 was knockdowned in stable HCC cell lines Hepa 1-6/PGLYRP2 and Huh7/PGLYRP2. The expression levels of PGLYRP2 and CCL5 in PGLYRP2 or CCL5 silenced stable cell lines Hepa 1-6/PGLYRP2 (A) and Huh7/PGLYRP2 (B) were detected by Real-time PCR. (C) The expression levels of PGLYRP2 and CCL5 in PGLYRP2 or CCL5 silenced stable cell lines Hepa 1-6/PGLYRP2 and Huh7/PGLYRP2 were detected by Western blot. (D) MTT assay of PBMC/Huh7 (Con, PGLYRP2 or PGLYRP2+siPGLYRP2) co-culture system was performed. (E) The cytotoxicity assay of PBMCs on tumor cells was analyzed by incubating PBMCs with Huh7/Con or Huh7/PGLYRP2 with or without 1 μg/ml CCL5 blocking antibody (53405.111, ab10394, Abcam, Cambridge, UK) for 2 h, 4 h and 8 h at an E:T ratio of 10:1. (F) Survival rate of PBMC/Huh7 (Con, PGLYRP2 or PGLYRP2+siPGLYRP2) xenografted BALB/c-nu/nu mice were performed. The results represent at least three independent

experiments and are reported as mean ± SEM. *, $p<0.05$; **, $p<0.001$; ns, not significant.

Fig. S7 Identification of immune effector cells of PGLYRP2-mediated anti-tumor immunity (A) Depletion of immune cells by intraperitoneally administering 200 μg of depleting antibody i.p. twice weekly beginning one day prior to tumor injection. 1×10^6 stable Hepa 1-6/PGLYRP2 cells and control cells were injected subcutaneously into the right posterior flanks of 6-week-old immune-competent BALB/c mice. Tumor weight was measured at the end of the sudy. The depletion of immune cells was confirmed by using flow cytometry analysis. (B) The tumor killing activity of five independent PBMC donors was verified in PBMC-K562 co-culture system at an E:T ratio of 10:1. Cytotoxicity was measured after 2 h, 4 h and 8 h of incubation. (C) Cytotoxicity assay of NK cell line NK-92 was analyzed by incubating target cells Huh7/Con or Huh7/PGLYRP2 with NK92 for 2 h and 4 h at an E:T ratio of 10:1. (D, E) Cytotoxicity assay of cultured NK cells was analyzed by incubating target cells K562 (D), Huh7/Con or Huh7/PGLYRP2 (E) with cultured NK cells for 2 h and 4 h at an E:T ratio of 10:1. (F) Cell subsets of PBMC from healthy donor were identified by flow cytometry. (G) Cell subsets of cultured NK cells (NK-1, NK-2 and NK-3) from healthy donors were identified by flow cytometry. All the results are reported as mean ± SEM. *, $p<0.05$; **, $p<0.001$; ns, not significant.

Fig. S8 Apoptosis assay of PGLYRP2-overexpressed Huh7 and Hepa1-6 cells. (A) Apoptosis assay was performed with Annexin V-FITC/PI staining in stable Huh7/PGLYRP2, Hepa1-6/PGLYRP2 and corresponding control cells. (B) Statistic analysis showed the percentage of both early (Annexin V+/PI−) and late (Annexin V+/PI+) apoptotic cells. Student's t test was used to compare values. The results represent at least three independent experiments and are reported as mean ± SEM. The ns indicates there is no significant difference.

Table S1 Clinicopathologic features of PGLYRP2 expression in HCC

Indexes	Total number	PGLYRP2 expression level		*P* value
		High（n=27）	Low (n=46)	
Average age				0.740
≥55	36	14	22	
<55	37	13	24	
Sex				0.751
Male	61	22	39	
Female	12	5	7	
Cirrhosis				0.312
Yes	27	12	15	
No	46	15	31	
Tumor size				0.008*
≤5 cm	31	17	14	
>5 cm	42	10	32	
Tumor number				0.847
=1	67	25	42	
>1	6	2	4	
Histological grade				0.011*
I, I-II	9	7	2	
II, II-III, III	64	20	44	
TNM stage				0.008*
I-II	39	20	19	
III-IV	34	7	27	

Note：- and + staining intensities indicate low level of PGLYRP2 expression; ++ and +++ staining intensities indicate high expression level. *A *p*-value<0.05 was considered statistically significant. The *p*-values were calculated using Fisher's test.

Table S2 Clinical data on the specimen used in IHC, cDNA array and methylation status analysis of PGLYRP2 promoter

1. HCC tissue array HLiv-HCC180Sur-01

tissue code	Gender	Age	Life time	Pathological typing	Histological grade	TNM stage	Tumor size (cm)
RDgLiv0704A0186	Male	67	79	Hepatocellular carcinoma	Ⅰ-Ⅱ	T2N0M0	3×2.5×2
RDgLiv0706A0222	Male	62	77	Hepatocellular carcinoma	Ⅰ-Ⅱ	T2N0M0	4.5×4×3
RDgLiv0706A0228	Female	50	11	Hepatocellular carcinoma	Ⅱ-Ⅲ	T2N0M0	5.5×5×4
RDgLiv0709A0236	Male	57	43	Hepatocellular carcinoma，with cirrhosis	Ⅱ-Ⅲ	T2N0M0	4×3.5×3
RDgLiv0709A0239	Male	56	32	Hepatocellular carcinoma，with cirrhosis	Ⅱ	T2N0M0	1×1×1, 3×3×3
RDgLiv0710A0240	Female	54	73	Hepatocellular carcinoma，with cirrhosis	Ⅱ	T2N0M0	2×1.5×1.5, 1.5×1.5×1
RDgLiv0803A0328	Male	46	16	Hepatocellular carcinoma	Ⅲ	T3N0M0	18×13×7
RDgLiv0803A0329	Male	52	66	Hepatocellular carcinoma	Ⅲ	T3N0M0	16×14×6
RDgLiv0807A0380	Male	61	62	Hepatocellular carcinoma	Ⅰ-Ⅱ	T1N0M0	1.5×1.5×1
RDgLiv0812A0413	Male	54	57	Hepatocellular carcinoma	Ⅱ	T2N0M0	3.5×3×2.5
RDgLiv0812A0414	Male	48	57	Hepatocellular carcinoma	Ⅰ	T2N0M0	6×5.5×5
RDgLiv0901A0432	Female	65	57	Hepatocellular carcinoma，with cirrhosis	Ⅱ	T2N0M0	7×4×4
RDgLiv0904A0464	Male	52	55	Hepatocellular carcinoma	Ⅲ	T3N0M0	9×5×3
RDgLiv0904A0469	Male	55	55	Hepatocellular carcinoma	Ⅱ	T2N0M0	7×6×5
D19A0561	Male	40	50	Hepatocellular carcinoma，with cirrhosis	Ⅱ-Ⅲ	T3N0M0	9.5×8×5
D19A0562	Male	59	50	Hepatocellular carcinoma	Ⅱ-Ⅲ	T3N0M0	13×12×10
D19A0582	Male	63	49	Hepatocellular carcinoma	Ⅰ-Ⅱ	T2N0M0	7.5×5×4.5

D19A0690	Male	65	35	Hepatocellular carcinoma	II	T2N0M0	7×5×5
D19A0695	Male	47	46	Hepatocellular carcinoma	II	T2N0M0	4×3.5×3.5
D19A0715	Male	56	44	Hepatocellular carcinoma，with cirrhosis	I	T2N0M0	5×5×3
D19A0860	Female	71	41	Hepatocellular carcinoma，with cirrhosis	II	T2N0M0	4.5×4.5×4
D19A0867	Male	46	19	Hepatocellular carcinoma	III	T2N0M0	5.5×4.5×2.5
D19A1169	Male	73	32	Hepatocellular carcinoma	I-II	T3N0M0	11×9×7
D19A0931	Male	62	39	Hepatocellular carcinoma	II-III	T2N0M0	3.5×3×3
D19A1287	Male	72	37	Hepatocellular carcinoma，with cirrhosis	II	T1N0M0	3×2×2
D19A1293	Female	47	37	Hepatocellular carcinoma	II-III	T2N0M0	7.5×5.5×4.5
D19A1311	Male	53	20	Hepatocellular carcinoma	II	T3N0M0	10×6×4
RDgLiv0704A0179	Male	45	80	Hepatocellular carcinoma	II-III	T3N0M0	3×2.5×2
RDgLiv0704A0187	Male	65	11	Hepatocellular carcinoma	II-III	T3N0M0	9×8×8
RDgLiv0704A0192	Male	38	39	Hepatocellular carcinoma	III	T3N0M1	3×2.5×2
RDgLiv0704A0195	Male	58	78	Hepatocellular carcinoma	II-III	T2N0M0	14×10×7
RDgLiv0704A0207	Male	40	77	Hepatocellular carcinoma	II-III	T1N0M0	1.8×1.5×1.2
RDgLiv0704A0211	Male	70	13	Hepatocellular carcinoma	II	T3N1M0	12×7.5×6
RDgLiv0706A0220	Male	55	49	Hepatocellular carcinoma	I-II	T3N0M0	15×8.5×6.5
RDgLiv0706A0231	Male	56	4	Hepatocellular carcinoma	III	T3N0M0	1×1×1, 7×5×5
RDgLiv0710A0241	Male	51	29	Hepatocellular carcinoma	III	T2N0M0	5.5×5.5×3.5
RDgLiv0710A0244	Female	58	73	Hepatocellular carcinoma，with cirrhosis	II	T1N0M0	2.5×2.5×2

RDgLiv0710A0256	Male	50	73	Hepatocellular carcinoma	II	T2N0M0	6×6×5.5
RDgLiv0710A0258	Female	57	2	Hepatocellular carcinoma，with cirrhosis	II-III	T2N0M0	4×3.5×3
RDgLiv0801A0314	Male	57	29	Hepatocellular carcinoma	III	T2N0M0	4×4×4, 3×3×3
RDgLiv0802A0319	Male	52	35	Hepatocellular carcinoma，with cirrhosis	II	T3N0M0	30×15×10
RDgLiv0802A0323	Male	43	67	Hepatocellular carcinoma	II	T1N0M0	1.5×1×1
RDgLiv0802A0325	Female	48	25	Hepatocellular carcinoma	II	T3N0M0	11×6×6
RDgLiv0802A0327	Male	56	4	Hepatocellular carcinoma	III	T4N0M0	13×7×4
RDgLiv0803A0330	Male	52	16	Hepatocellular carcinoma	III	T3N0M0	6×6×6
RDgLiv0804A0336	Male	56	6	Hepatocellular carcinoma	III	T3N0M0	13×11×5
RDgLiv0804A0338	Male	54	17	Hepatocellular carcinoma	II	T2N0M0	4.5×4.5×4
RDgLiv0804A0340	Male	57	11	Hepatocellular carcinoma，with cirrhosis	II-III	T4N0M0	19×18×10
RDgLiv0804A0343	Male	56	14	Hepatocellular carcinoma，with cirrhosis	I	T2N0M0	4×4×4
RDgLiv0806A0363	Female	72	4	Hepatocellular carcinoma	II-III	T3N0M0	11×6×5
RDgLiv0806A0365	Male	43	4	Hepatocellular carcinoma，with cirrhosis	II	T3N0M0	15×13×9
RDgLiv0808A0385	Male	49	5	Hepatocellular carcinoma，with cirrhosis	III	T3N0M0	9×6×4, 2.8×2.5×1
RDgLiv0808A0388	Male	68	1	Hepatocellular carcinoma，with cirrhosis	III	T3N0M0	12×9×9
RDgLiv0811A0403	Male	42	3	Hepatocellular carcinoma，with cirrhosis	II	T1N0M0	2×1.5×1.5
RDgLiv0811A0407	Female	51	22	Hepatocellular carcinoma，	II	T3N0M0	5.5×5.5×3, 1.5×1.3×1.3

				with cirrhosis			
RDgLiv0901A0436	Male	51	17	Hepatocellular carcinoma，with cirrhosis	Ⅱ	T3N0M0	10×7×7
RDgLiv0902A0454	Male	52	30	Hepatocellular carcinoma	Ⅱ	T3N0M0	14×10×10
RDgLiv0904A0463	Male	57	32	Hepatocellular carcinoma	Ⅲ	T3N0M0	14×9×6
RDgLiv0904A0471	Male	54	54	Hepatocellular carcinoma	Ⅱ	T2N0M0	3×2.5×1.7
RDgLiv0904A0472	Male	51	5	Hepatocellular carcinoma	Ⅱ	T2N0M0	3.5×3×2.5
RDgLiv0904A0475	Female	54	16	Hepatocellular carcinoma	Ⅱ	T2N0M0	3×3×2
RDgLiv0904A0487	Male	65	4	Hepatocellular carcinoma	Ⅱ	T3N0M0	13×10×4
RDgLiv0904A0488	Female	67	54	Hepatocellular carcinoma	Ⅱ	T2N0M0	4×4×3
RDgLiv0904A0490	Male	54	6	Hepatocellular carcinoma	Ⅱ	T3N0M0	3×2.5×2
RDgLiv0905A0510	Male	56	4	Hepatocellular carcinoma	Ⅱ-Ⅲ	T3N0M0	7×4.5×3
D19A0567	Male	40	5	Hepatocellular carcinoma，with cirrhosis	Ⅱ	T3N0M0	22×12×6
D19A0623	Male	73	47	Hepatocellular carcinoma	Ⅱ	T1N0M0	3×3×3
D19A0628	Male	56	5	Hepatocellular carcinoma	Ⅱ	T2N0M0	4×4×2.5
D19A0689	Male	38	16	Hepatocellular carcinoma	Ⅱ	T3N0M0	3×4×3
D19A0835	Male	50	2	Hepatocellular carcinoma	Ⅱ	T3N0M0	13×11×8
D19A0856	Male	56	37	Hepatocellular carcinoma	Ⅱ	T3N0M0	6.5×5×4
D19A1173	Male	53	38	Hepatocellular carcinoma，with cirrhosis	Ⅱ	T2N0M0	6×5×4
D19A1179	Male	63	12	Hepatocellular carcinoma	Ⅱ-Ⅲ	T2N0M0	4×3×2.5

2. HCC tissue array Hliv-HCC030PG-01

Tissue code	Gender	Age	Pathological typing	Histological grade	Primary organ	Tumor size (cm)
CDgLiv0506A0092	Male	61	Hepatocellular carcinoma	Ⅰ - Ⅱ	Yes	4×4×3
CDgLiv0811A0423	Male	63	Hepatocellular carcinoma	Ⅰ - Ⅱ	Yes	4.5×3.5×3
CDgLiv0901A0443	Male	64	Hepatocellular carcinoma	Ⅰ - Ⅱ	Yes	7×7×5
CDgLiv0707A0251	Male	64	Hepatocellular carcinoma	Ⅱ	Yes	11×9×2
CDgLiv0709A0270	Male	34	Hepatocellular carcinoma	Ⅱ	Yes	5×4×4
CDgLiv0711A0293	Male	43	Hepatocellular carcinoma	Ⅱ	Yes	3.4×3.2×2.1
CDgLiv0801A0317	Male	52	Hepatocellular carcinoma	Ⅱ	Yes	4×3.8
CDgLiv0803A0346	Female	63	Hepatocellular carcinoma	Ⅱ	Yes	4×3×3
CDgLiv0812A0439	Female	56	Hepatocellular carcinoma	Ⅱ	Yes	6×4×4
CDgLiv0901A0442	Male	63	Hepatocellular carcinoma	Ⅱ	Yes	3.5×3×3
CDgLiv0902A0459	Male	53	Hepatocellular carcinoma	Ⅱ	Yes	3.2×3×3
CDgLiv0904A0481	Male	52	Hepatocellular carcinoma	Ⅱ	Yes	10×7×6
CDgLiv0806A0373	Male	42	Hepatocellular carcinoma	Ⅱ - Ⅲ	Yes	6×5×5
CDgLiv0711A0289	Female	68	Hepatocellular carcinoma	Ⅲ	Yes	4.5×4×4
CDgLiv0711A0291	Male	55	Hepatocellular carcinoma	Ⅲ	Yes	6×6×5

3. HCC tissue array HLivH090Su01

Tissue code	Gender	Age	Pathological typing	Histological grade	Distant transfer	Primary organ	Tumor size (cm)
D19A1249	Male	53	Hepatocellular carcinoma	III	No	Yes	6.5×5.5×5.5
D19A1251	Male	45	Hepatocellular carcinoma	II	No	Yes	8×7.9×7
D19A1253	Male	53	Hepatocellular carcinoma	II	No	Yes	17×16×9
D19A1254	Male	49	Hepatocellular carcinoma	III	No	Yes	9×7×7
D19A1261	Male	39	Hepatocellular carcinoma	II	No	Yes	8.5×8×6
D19A1263	Male	51	Hepatocellular carcinoma	Ⅰ-II	No	Yes	7×6×6
D19A1266	Male	69	Hepatocellular carcinoma	II	No	Yes	8×6×6
D19A1267	Male	44	Hepatocellular carcinoma	II	No	Yes	4.5×4.5×3
D19A1203	Female	58	Hepatocellular carcinoma	Ⅰ-II	No	Yes	4.7×4×4
D19A1269	Male	51	Hepatocellular carcinoma	Ⅰ-II	No	Yes	5×4×3
D19A1802	Male	45	Hepatocellular carcinoma	II	No	Yes	4×4×3
D19A1800	Male	51	Hepatocellular carcinoma	III	No	Yes	2.5×2×2
D19A1798	Female	48	Hepatocellular carcinoma	II	No	Yes	3.5×3×3
D19A1799	Male	63	Hepatocellular carcinoma	II-III	No	Yes	7×5.5×5

4. HCC tissue array OD-CT-DgLiv02-005

Tissue code	Gender	Age	Pathological typing	Histological grade	Distant transfer	Primary organ	Tumor size
CDgLiv0801A0344	Female	59	Hepatocellular carcinoma	Ⅰ	No	Yes	5×5×5cm
CDgLiv0704A0204	Female	57	Hepatocellular carcinoma	Ⅰ-Ⅱ	No	Yes	7×8×7cm
CDgLiv0711A0292	Male	45	Hepatocellular carcinoma	Ⅰ-Ⅱ	No	Yes	2×2×2cm
CDgLiv0804A0369	Male	61	Hepatocellular carcinoma	Ⅰ-Ⅱ	No	Yes	2.2×1.2×1.2cm
CDgLiv0704A0197	Male	71	Hepatocellular carcinoma	Ⅱ	No	Yes	2.5×2.5×2cm
CDgLiv0704A0200	Male	53	Hepatocellular carcinoma	Ⅱ	No	Yes	3×3×3cm
CDgLiv0803A0348	Male	50	Hepatocellular carcinoma	Ⅱ	No	Yes	9×7×6cm
CDgLiv0709A0255	Male	32	Hepatocellular carcinoma	Ⅱ-Ⅲ	No	Yes	8×5.5×6cm
CDgLiv0712A0298	Male	38	Hepatocellular carcinoma	Ⅲ	No	Yes	11×9×5cm
CDgLiv0804A0368	Male	71	Hepatocellular carcinoma	Ⅲ	No	Yes	4×2.5×2cm

5. cDNA array cDNA-HlivH60PG02

Tissue code	Gender	Age	Pathological typing	Histological grade	TNM stage	History of liver disease	Tumor size (cm)
D19A1531	Male	61	Hepatocellular carcinoma	Ⅱ	T3N0M0	Cirrhosis, Hepatitis B	3×5 , 5×6
D19A1541	Male	41	Hepatocellular carcinoma	Ⅱ	T2N0M0	Cirrhosis, Hepatitis B	2×3
D19A1545	Male	53	Hepatocellular carcinoma	Ⅱ	T3N0M0	Cirrhosis, Hepatitis B	4×4×5, 5.5×3×1.5
D19A1754	Female	23	Hepatocellular carcinoma	Ⅱ	T2N0M0		9
D19A2384	Male	70	Hepatocellular carcinoma	Ⅱ	T3N0M0	Cirrhosis, Hepatitis B	6
D19A2388	Male	62	Hepatocellular carcinoma	Ⅱ	T2N0M0	Cirrhosis, Hepatitis B	7
D19A2411	Male	42	Hepatocellular carcinoma	Ⅱ	T2N0M0	Cirrhosis, Hepatitis B	5×4×4
D19A1144	Male	47	Hepatocellular carcinoma	Ⅱ-Ⅲ	T2N0M0	Hepatitis B	13.2×8.6
D19A1370	Male	41	Hepatocellular carcinoma	Ⅱ-Ⅲ	T2N0M0		5×4.5×4
D19A1525	Male	68	Hepatocellular carcinoma	Ⅱ-Ⅲ	T2N0M0	Cirrhosis, Hepatitis B	7
D19A1532	Male	62	Hepatocellular carcinoma	Ⅱ-Ⅲ	T2N0M0	Cirrhosis, Hepatitis B	6
D19A2079	Male	53	Hepatocellular carcinoma	Ⅱ-Ⅲ	T3N0M0	Cirrhosis, Hepatitis B	7
D19A2091	Female	69	Hepatocellular carcinoma	Ⅱ-Ⅲ	T3N0M0	Cirrhosis, Hepatitis B	7
D19A2331	Male	59	Hepatocellular carcinoma	Ⅱ-Ⅲ	T2N0M0		4.5×4.5×4
D19A2335	Female	60	Hepatocellular carcinoma	Ⅱ-Ⅲ	T2N0M0		4×3×3
D19A2392	Male	53	Hepatocellular carcinoma	Ⅱ-Ⅲ	T2N0M0	Cirrhosis, Hepatitis B	10×8
D19A2404	Female	65	Hepatocellular carcinoma	Ⅱ-Ⅲ	T3N0M0	Cirrhosis, Hepatitis B	7
D19A2406	Male	55	Hepatocellular carcinoma	Ⅱ-Ⅲ	T2N0M0	Cirrhosis, Hepatitis B	6
729406/12-29	Male	66	Hepatocellular carcinoma	Ⅱ-Ⅲ	T2N0M0		1.5
744588/12-471	Male	73	Hepatocellular carcinoma	Ⅱ-Ⅲ	T2N0M0		2.5

D19A2634	Female	54	Hepatocellular carcinoma	Ⅲ	T4N0M1		12×13
D19A0886	Male	42	Hepatocellular carcinoma	Ⅳ	T4N0M0	Hepatitis B	7.1×5

6. three HCC samples used in analysis of methylation status of PGLYRP2 promoter

Patient	Tumor_type	Gender	Age_at_initial_pathologic_diagnosis	Histological_type	Primary_tumor_pathologic_spread
HCC001	Primary liver cancer	MALE	59	Hepatocellular Carcinoma	Invasive type, differentiated adenocarcinoma
HCC002	Primary liver cancer	FEMALE	62	Hepatocellular Carcinoma	Invasive type, differentiated adenocarcinoma
HCC003	Primary liver cancer	MALE	40	Hepatocellular Carcinoma	Invasive type, differentiated adenocarcinoma

Tumor_stage	History_of_hepatitis b infection	history_of_hepatitis c infection	alcohol consumption	AFP level	vital_status	Written informed consent for publication of their clinical details
T4aN0M0; IIB	NO	NO	YES	400	LIVING	YES
T4N1M0; III	YES	NO	NO	218	DEAD	YES
T4N1M1; III	YES	YES	YES	3510	DEAD	YES

Table S3 Primer sets and siRNA sequences

Primer sets for Bisulfite DNA sequencing

Primer name	Sequence
PGLYRP2 promoter 33F	5'-TATTTGAGGTTGGGAGTTTGAGATTAG-3'
PGLYRP2 promoter 767R	5'-GGGGTTGAGTTTGAGTGTTTAGGAT-3'
PGLYRP2 promoter 671F	5'-AGGTGGAGGTTGTAGTGAGTTGAGAT-3'
PGLYRP2 promoter 1295R	5'-TGTGGGTTGAGGTAGGGATTAGG-3'
PGLYRP2 promoter 1257F	5'-TTAGTTATGGGTATTTGGAGAAGAGGA-3'
PGLYRP2 promoter 2102R	5'-ATTTATTTGTTTTGGTTTTTTAAAGTGTTG-3'

Primer sets for immune markers

Primer name	Sequence
hCD3G RT_F	5’- GGAATCTGGGAAGTAATGCCAA-3’
hCD3G RT_R	5’- TCAATGCAGTTCTGACACATTCT-3’
hCD4 RT_F	5'-CTTCTGGTGCTGCAACTGG-3’
hCD4 RT_R	5'-GCTGTACAGGTCAGTTCC-3’
hCD8A RT_F	5'-CTTACCAGTGACCGCCTTG-3’
hCD8A RT_R	5'-CACTTCAGCTCCACTGTCTC-3’
Hcd14 RT_F	5'-GACCTAAAGATAACCGGCACC-3’
hCD14 RT_R	5'-GCAATGCTCAGTACCTTGAGG-3’
hCD68 RT_F	5'-GGAAATGCCACGGTTCATCCA-3’
hCD68 RT_R	5'-TGGGGTTCAGTACAGAGATGC-3’
hCD22 RT_F	5'-CACCTCAATGACAGTGGTCAG-3’
hCD22 RT_R	5'-TGGATCGGATACCCATAGCAG-3’
hCD11b RT_F	5'-ACTTGCAGTGAGAACACGTATG-3’
hCD11b RT_R	5'-TCATCCGCCGAAAGTCATGTG-3’
hFOXP3 RT_F	5'-GTGGCCCGGATGTGAGAAG-3’
hFOXP3 RT_R	5'-GGAGCCCTTGTCGGATGATG-3’
C2 RT_F	5'-CCTTGAATGGGAGCAAACTGAAC-3’
C2 RT_R	5'-GATTGATGTGAAAGTCTCGTGGC-3’
C3 RT_F	5'-GCTGCTCCTGCTACTAACCCA-3’
C3 RT_R	5'-AAAGGCAGTTCCCTCCACTTT-3’

Primer sets for chemokines

Primer name	Sequence
CCL5 RT_F	5'-CCAGCAGTCGTCTTTGTCAC-3’
CCL5 RT_R	5'-CTCTGGGTTGGCACACACTT-3’
Midkine RT_F	5'-CGCGGTCGCCAAAAAGAAAG-3’
Midkine RT_R	5'-TACTTGCAGTCGGCTCCAAAC-3’
CXCL7 RT_F	5'-GTAACAGTGCGAGACCACTTC-3’
CXCL7 RT_R	5'-CTTTGCCTTTCGCCAAGTTTC-3’
CXCL4 RT_F	5'-GTCCGTCCCAGGCACATCA-3’
CXCL4 RT_R	5'-GCTTGCAGGTCCAAGCAAATT-3’

CXCL12 RT_F	5'-ATTCTCAACACTCCAAACTGTGC-3’
CXCL12 RT_R	5'-ACTTTAGCTTCGGGTCAATGC-3’
CCL21 RT_F	5'-GTTGCCTCAAGTACAGCCAAA-3’
CCL21 RT_R	5'-AGAACAGGATAGCTGGGATGG-3’
Chemerin RT_F	5'-AGAAACCCGAGTGCAAAGTCA-3’
Chemerin RT_R	5'-AGAACTTGGGTCTCTATGGGG-3’
IL16 RT_F	5'-GCCGAAGACCCTTGGGTTAG-3’
IL16 RT_R	5'-GCTGGCATTGGGCTGTAGA-3’
Fibrinogen RT_F	5'-AGTGATTCAGAACCGTCAAGAC-3’
Fibrinogen RT_R	5'-CATCCTGGTAAGCTGGCTAATTT-3’

Primer sets for ChIP analysis

Primer name	Sequence
CCL5 promoter_F	5'-ATTCTATCACTGAGTGGGTGGA-3’
CCL5 promoter_R	5'-GTGTCATGGTGGTTTGCTGTA-3’
PGLYRP2 promoter-440F	5'-GGCATTTACTTACCTCTGGCTTTC-3’
PGLYRP2 promoter-315R	5'-GGGTCCTGGTTACATGGCTGT-3’
PGLYRP2 promoter-736F	5'-GTTTAGGATCTTATCTACCTCCATCA-3’
PGLYRP2 promoter-614R	5'-TCAACAAATGTTTCCCGAGTG-3’
PGLYRP2 promoter-1516F	5'-CAGCCTGGGAGACAGAGCA-3’
PGLYRP2 promoter-1362R	5'-GTGACGCAATCATGGTTCACT-3’
PGLYRP2 promoter-1741F	5'-CAGGCACGGTGGCTCAT-3’
PGLYRP2 promoter-1491R	5'-AGGGTCTTGCTCTGTCTCCC-3’

Primer sets for construction of promoter-luciferase reporter plasmids

Primer name	Sequence
CCL5 promoter luc -1841_KpnI F	5'-GGGGTACCCCCTGACTCTTGATTTCCTCCCG-3’
CCL5 promoter luc -500_KpnI F	5'-GGGGTACCCC AAGTGTCAGCATGTATCTACTAATAA-3’
CCL5 promoter luc -1_XhoI R	5'-CCGCTCGAGCGGGCAGAACGTGCAGGTTTGTT-3’
CCL5 promoter luc -500_XhoI R	5'-CCGCTCGAGCGGTTATTAGTAGATACATGCTGACACTT-3’
PGLYRP2 promoter luc_SacI F	5'-CGAGCTCGCATTGTCTTAGTTTGGGTCTTCC-3’
PGLYRP2 promoter luc_XhoI R	5'-CCGCTCGAGCGGCATGATTGTGGGTCACTGCA-3’

Primer sets for detection of mycoplasma contamination

Primer name	Sequence
Forward primers	
MF (for six species of mycoplasma)	5'-TCTGAAT(C/T)TGCCGGGACCACC-3'
PF (for M. pirum only)	5'-GGAAAATGTTATTTTGACGGAACCT-3'
AF (for A. laidlawii only)	5'-GGAATCCCGTTTGAAGATAGGA-3'
Reverse primer	
MR (for eight species of mycoplasma)	5'-CTTTCCATCACGGTACTGGTTCACT-3'

siRNA sequences

siRNA name	Sequence

siDNMT1_1	5'- GCAGGCGGCTCAAAGATTT-3'
siDNMT1_2	5'- GCTTCAGTGTGTACTGTAA-3'
siDNMT1_3	5'- GCTTCAATTCGCGCACCTA-3'
siDNMT3a_1	5'- CCATGTACCGCAAAGCCAT-3'
siDNMT3a_2	5'- CCAGATGTTCTTCGCTAAT-3'
siDNMT3a_3	5'- GCATCCACTGTGAATGATA-3'
siDNMT3b_1	5'- CCAAAGCTCTTCCGGGAAA-3'
siDNMT3b_2	5'- CCTCAAGACAAATTGCTAT-3'
siDNMT3b_3	5'- CCATGAAGGTTGGCGACAA-3'
siPGLYRP2_1	5'- GGCUGUACCACUUUCUGCUTT-3'
siPGLYRP2_2	5'- GACCAUGGCCUUCCUCAAUTT-3'
siPGLYRP2_3	5'- CCUGCUCUCCCAGUAUUAUTT-3'
siCCL5_1	5'- GCCCACGUCAAGGAGUAUUTT-3'
siCCL5_2	5'- CCAAUCUUGCAGUCGUGUUTT-3'
siCCL5_3	5'- GGGUUCAAGAAUACAUCAATT-3'

References

1. Shi M, Zhang Y, Liu L, Zhang T, Han F, Cleveland J, Wang F, et al. MAP1S Protein Regulates the Phagocytosis of Bacteria and Toll-like Receptor (TLR) Signaling. J Biol Chem 2016;291:1243-1250.

2. Shi M, Wang S, Yao Y, Li Y, Zhang H, Han F, Nie H, et al. Biological and clinical significance of epigenetic silencing of MARVELD1 gene in lung cancer. Sci Rep 2014;4:7545.

3. Narumi K, Miyakawa R, Ueda R, Hashimoto H, Yamamoto Y, Yoshida T, Aoki K. Proinflammatory Proteins S100A8/S100A9 Activate NK Cells via Interaction with RAGE. J Immunol 2015;194:5539-5548.

4. Zhang H, Hua Y, Jiang Z, Yue J, Shi M, Zhen X, Zhang X, et al. Cancer-associated Fibroblast-promoted LncRNA DNM3OS Confers Radioresistance by Regulating DNA Damage Response in Esophageal Squamous Cell Carcinoma. Clin Cancer Res 2018.